

# B. TECH. PROJECT REPORT

## On

# Stand-Alone PV System Design & Development

BY

Satyajeet Deshmukh

Himanshu Verma



**Department of Electrical Engineering  
Indian Institute of Technology Indore**

**May 2021**

Bachelor of Technology Project Report

# **Stand-Alone PV System Design & Development**

Submitted in partial fulfillment of the requirements for the award of the degree  
Bachelor of Technology in Electrical Engineering

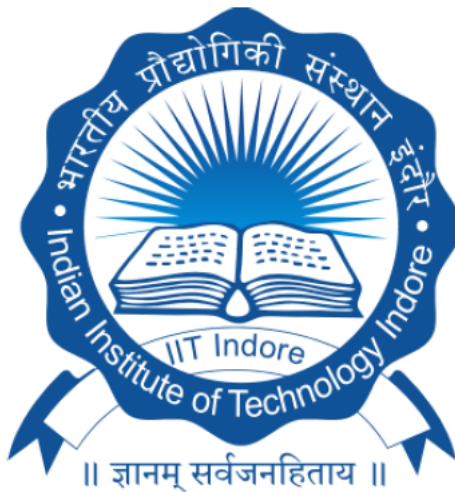
Submitted by

**Satyajeet Deshmukh    170002042**  
**Himanshu Verma       170002017**

Under the guidance of

**Dr. Amod C. Umarikar**

Associate Professor, Department of Electrical Engineering, IIT Indore



# Candidate's Declaration

We hereby declare that the project entitled "Stand-Alone PV System Design & Development" submitted in partial fulfillment for the award of the degree of Bachelor of Technology in Electrical Engineering completed under the supervision of Dr. Amod C. Umarikar, Associate Professor, IIT Indore is an authentic work.

Further, we declare that we have not submitted this work for the award of any other degree elsewhere.

Signature and name of the students with date:



Satyajeet  
26/05/21



Himanshu  
26/05/21

**Satyajeet Deshmukh** 170002042

**Himanshu Verma** 170002017

---

## Certificate by BTP Guide

It is certified that the above statement made by the students is correct to the best of my/our knowledge.

Signature of BTP Guide with dates and their designation:



29/05/2021

**Dr. Amod C. Umarikar**

Associate Professor

Department of Electrical Engineering, IIT Indore

# Acknowledgment

We would like to express our sincere gratitude to our project guide, Dr. Amod C. Umarikar for providing us the opportunity to work on this really interesting project and for his judicious guidance and generous support throughout the time.

We would also like to thank Suvamit Chakraborty, Ph.D. research scholar, for aiding us with his beneficent attitude and fruitful suggestions.

Special thanks to the IIT Indore administration and Covid Task Force for allowing us to return to the campus and complete our experimental project in a safe environment.

Sincerely,

Satyajeet Deshmukh & Himanshu Verma

B.Tech. IV Year

Discipline of Electrical Engineering

IIT Indore

# Abstract

This project aims at the design and hardware development of a single-phase standalone PV system. A boost converter and a bidirectional converter have been proposed for harnessing power from PV, storing and extracting energy from the battery, and connecting to loads at the DC-link. Solar Array Simulator is used as a pseudo PV source for hardware implementation along with two 12V Valve Regulated Lead Acid (VRLA) batteries as energy storage elements. The Arduino Mega 2560 is used as a microcontroller because it is cheap, simple, and easy to program. A setup of relay-based soft starter circuit, buffer circuits, current sensors, voltage sensors, digital isolators, and isolated gate drivers is connected to the Arduino to form the control subsystem. The details of the control system and software have been discussed in detail in the corresponding chapter. A working lab prototype was developed and its results were recorded. A PCB for the same was designed.

# Table of Contents

<b>Chapter 1 Introduction</b>	<b>1</b>
<b>Chapter 2 Converter Topology</b>	<b>3</b>
<b>PV Boost with Bidirectional DC-DC Converter</b>	<b>3</b>
<b>Chapter 3 Mathematical Model of PV Module</b>	<b>5</b>
<b>Chapter 4 Hardware Development</b>	<b>8</b>
4.1 Selection of Inductors	8
4.2 Selection of Capacitors	9
4.3 Selection of Switches	9
4.4 Selection of Gate Drivers	9
4.5 PV Simulator, Battery, and Loads	10
4.6 Designing of Sensing Circuits	10
4.6.1 Voltage sensor	10
4.6.2 Current sensor	11
4.7 Soft Starter Circuit	12
4.8 Relay selection	14
4.9 Fuse Selection	14
4.10 Hardware Prototype Photos	15
<b>Chapter 5 Control Scheme and Software</b>	<b>18</b>
5.1 Modes of Operation	18
5.1.1 MPPT Mode	18
5.1.2 Battery-Only (BO) Mode	19
5.1.3 Non-MPPT Mode	20
5.2 MPPT Algorithm: Perturb and Observe (P&O)	21
5.3 Control System	22

5.3.1 Duty Cycle Control System:	22
5.3.2 Mode Selector System:	24
5.4 Overview of Software Development	25
5.5 Working of the Code	26
5.5.1 Global Variables	27
5.5.2 User-defined Functions	27
<b>Chapter 6 PCB Design</b>	<b>31</b>
<b>Chapter 7 Results</b>	<b>35</b>
7.1 Experimental results	35
7.1.A Battery-Only (BO) mode	35
7.1.B MPPT Mode	37
7.1.C NON-MPPT Mode	39
<b>Chapter 8 Conclusions and Future Work</b>	<b>41</b>
<b>References</b>	<b>43</b>

# List of figures

Fig. 1.1. Schematic Block Diagram of Stand Alone PV Based Systems	2
Fig. 2.1. Schematic Block Diagram of Converter Topology	3
Fig. 2.2. Schematic Circuit Diagram of Converter Topology	4
Fig. 3.1. Equivalent Circuit of a Solar Cell	6
Fig. 3.2. I-V characteristics at different isolation levels	7
Fig. 3.3. P-V characteristics at different isolation levels	7
Fig. 3.4. I-V characteristics at different temperature values	7
Fig. 3.5. P-V characteristics at different temperature values	7
Fig. 4.1. Schematic diagram of Voltage sensor	11
Fig. 4.2. Schematic diagram of ACS712	12
Fig. 4.3. Circuit diagram of Soft Start	13
Fig. 4.4. Complete Circuit	15
Fig. 4.5. Voltage Sensor	15
Fig. 4.6. Complete Setup	16
Fig. 4.7. Soft Starter	16
Fig. 4.8. Bi-directional Converter	16
Fig. 5.1.1.1 Power Flow in MPPT Mode	18
Fig. 5.1.2.1 Power Flow in BO mode	19
Fig. 5.1.3.1 Power Flow in non-MPPT mode	20
Fig. 5.2.a Block control system diagram of P&O mode	22
Fig. 5.2.b Power-Voltage hill climb representation in P&O algorithm	22
Fig. 5.3.1.1 Control system block diagram for boost and high side duty cycle	23
Fig. 5.3.1.2 Control system block diagram for low side duty cycle	24
Fig. 5.3.2.3 Control system block diagram for Mode Selector in MPPT Mode	25
Fig. 5.3.2.4 Control system block diagram for Mode Selector in non-MPPT Mode	25
Fig. 5.5.1 Block diagram of basic code structure in Arduino	27
Fig. 5.5.2 Block diagram of setup()	27
Fig. 5.5.3 Block Diagram of Loop before Relay is turn ON (Pre Soft-Start)	30

Fig. 5.5.4 Block Diagram of Loop after Relay is switched ON (Soft-Start Mode)	30
Fig. 6.1 Key points of consideration in PCB Design	31
Fig. 6.2 PCB Frontside	32
Fig. 6.3 PCB Backside	33
Fig. 6.4 PCB Footprint	34
Fig. 7.1.A.1 Full waveform in BO mode	35
Fig. 7.1.A.2 Soft start waveform in BO mode	36
Fig. 7.1.A.3 Steady State waveform in BO mode	36
Fig. 7.1.A.4 Steady State Current Ripple in BO mode	37
Fig. 7.1.B.1 Full waveform for Charging to Discharging of battery in MPPT Mode on load change	38
Fig. 7.1.B.2 Full waveform for mode switching from BO to MPPT to BO	39
Fig. 7.1.C.1 Full waveform for mode switching from MPPT to non-MPPT to MPPT	40
Fig. 8.1 Block diagram of modified non-MPPT Control system	42

# Chapter 1 Introduction

PV systems meant for acting as a power supply require an auxiliary power source in form of battery, supercapacitor, fuel cell, wind generator, or maybe grid, if possible. The output power of PV modules varies widely with changes in solar irradiation and temperature. PV systems meant for small or low power applications generally exhibit relatively high power capacity at high levels of irradiation and very low power capacity at low levels of irradiation. So an economic design of a PV-based power generation system requires an energy storage element in the form of a battery. [1] For rural household applications where the power supply changes widely with the changes in atmospheric conditions, choosing a battery for an energy storage scheme is an effective choice. Rural Household applications generally involve ac power-driven appliances while the output power of PV or battery is dc in nature. PV could power stand-alone appliances, instruments, and devices in cities and remote areas. [1] Parking meters, temporary traffic signs, emergency phones, radio transmitters, water irrigation pumps, stream-flow gauges, remote guard posts, roadway lighting, and more will all benefit from PV. [2] Hence, there is a need for an efficient and reliable electrical power conversion system.

The scope of the project work involves integration, analysis, simulation, and hardware implementation of a reliable, efficient, and cost-effective DC-DC standalone system. This DC-DC standalone system then can be integrated with an inverter to satisfy the household energy requirements.

Past research endeavors on stand-alone PV-based applications investigated many different topologies and control schemes for integrating PV modules with battery and load. Designing a PV system with a battery requires effective battery charging and discharging control so as not to affect battery life and health. Battery life and health deteriorate if an unregulated current is drawn from or supplied to the battery. A general block diagram of the stand-alone PV system is shown in Fig. 1.1.

The work included in this thesis proposes a configuration using a boost inverter with a bidirectional dc-dc converter. Converter analysis of boost converter and bidirectional dc-dc converter is presented in chapter 2. Modeling of a solar array of 17.6V along with PV and Battery sizing has been presented in chapter 3. Details of the hardware prototype built are presented in chapter 4. The control scheme employed for the proposed configuration is presented in chapter 5. Detailed simulation and hardware results are presented in chapter 7.

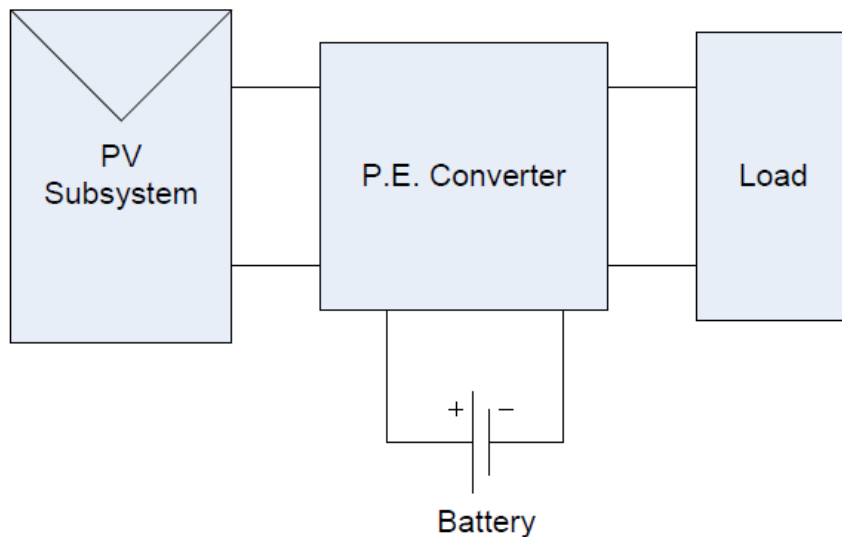


Fig. 1.1. Schematic Block Diagram of Stand Alone PV Based Systems

# Chapter 2 Converter Topology

## PV Boost with Bidirectional DC-DC Converter

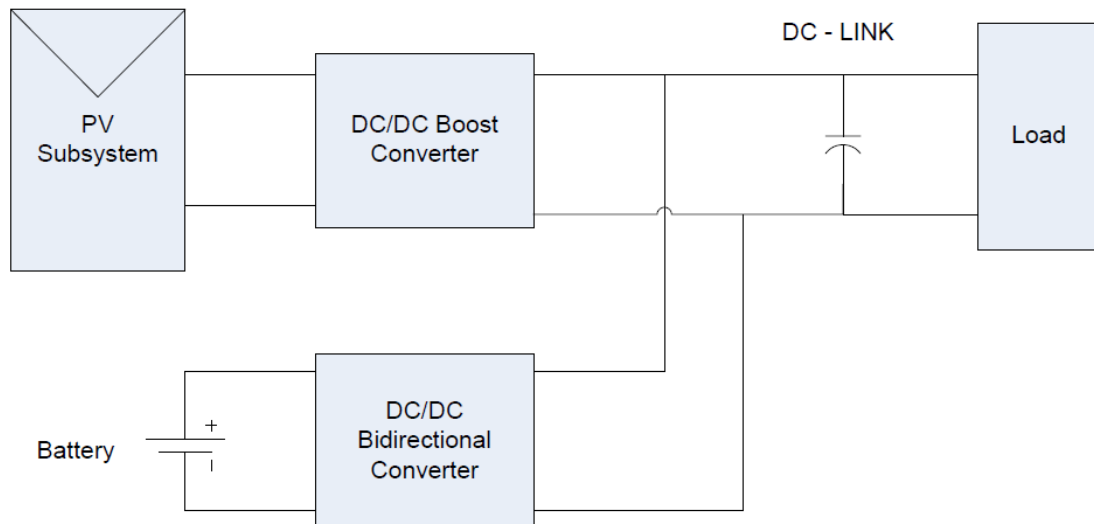


Fig. 2.1. Schematic Block Diagram of Converter Topology

As seen in Fig 2.1 the converter topology consists of 2 main components: DC-DC Boost and DC-DC Bidirectional converters. Both operate in a coordinated manner to maintain the DC-Link voltage at a constant voltage. The use of a bidirectional DC-DC converter allows for control over the charging and discharging currents into the battery. Fig 2.2 reveals the components inside the converters.

The MOSFETs M<sub>2</sub>, M<sub>3</sub> in the bidirectional converter are operated using complementary Pulse Width Modulation (PWM) signals. MOSFET M<sub>1</sub> is operated independently to control the boost subsystem. According to the sign convention, the charging battery current is positive and the discharging current is negative. The current coming out from the PV subsystem is positive. The current being supplied to the load is positive. This sign convention will be followed throughout the thesis.

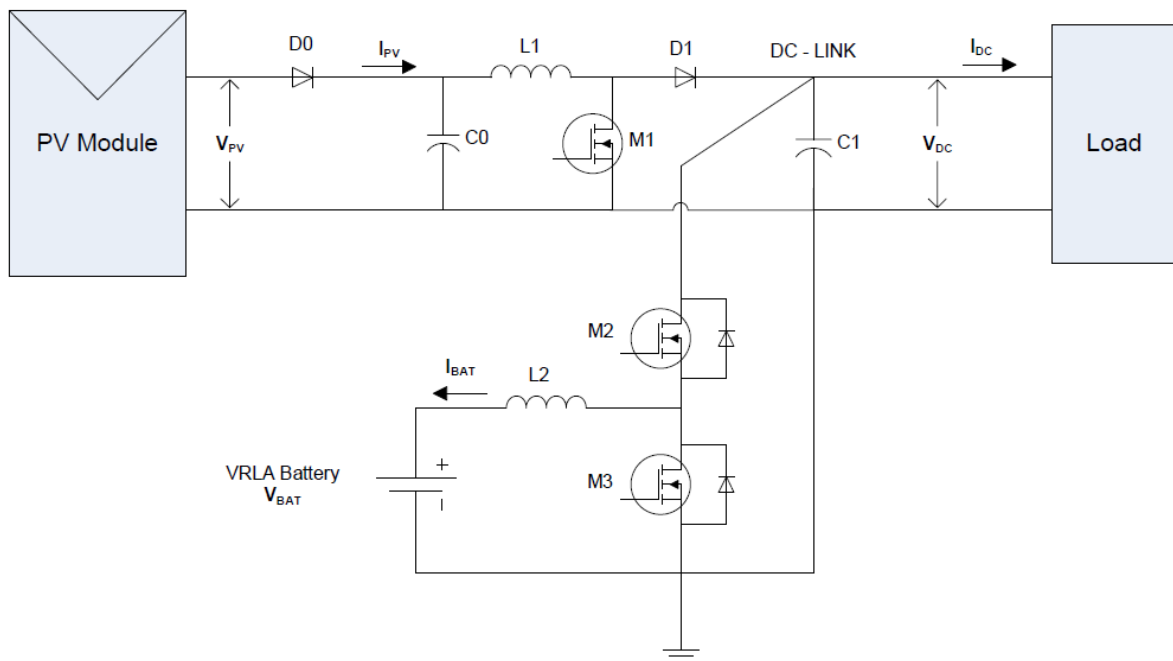


Fig. 2.2. Schematic Circuit Diagram of Converter Topology

- $V_{PV}$  : Voltage across the PV Module
- $I_{PV}$  : Current flowing out of the PV Module
- $V_{BAT}$  : Voltage of the Battery
- $I_{BAT}$  : Current flowing into the Battery
- $V_{DC}$  : Voltage across the DC-Link Capacitor
- $I_{DC}$  : Current flowing into the Load

During charging of the battery, the power is drawn from the DC-Link to the battery and vice-versa while discharging. The power transfer in boost is always from PV to the DC-Link. The exchange of power is managed using a control scheme such that the DC-Link remains voltage regulated. Thus the power is balanced as  $P_{PV} = P_{BAT} + P_{LOAD}$ .

$P_{BAT}$  is positive when the battery is charging because of our sign convention for battery current being positive while charging.

# Chapter 3 Mathematical Model of PV Module

To design a PV system it is necessary to select a PV module with high power capacity at MPP. A mathematical model of a solar module can be created, whose specifications are provided below:

Maximum Power  $P_m$ : 34W

Open circuit voltage: 21.7V

Short circuit current: 2.1A

Maximum power voltage: 17.5V

Maximum power current: 1.95A

For our project, we chose this solar module for final testing. But unfortunately, due to covid-19 spread inside the campus, labs were closed so we were unable to perform on this module. For simulation purposes, the mathematical model of the solar array has been built from the solar cell characteristics as depicted. The modeling of a solar array is given below:

$q$  = charge of an electron =  $1.6 \times 10^{-19}$  Coulomb

$k$  = Boltzmann's Constant =  $1.38 \times 10^{-23}$  J/K

$T_{aC}$  = ambient temperature = 25°C

$T_{aK}$  = operating temperature in K =  $273 + T_{aC}$

$A$  = 1(ideality factor)

$n$  = 1.2(diode quality factor)

$T_1$  = standard operating temperature = 25°C

$T_2$  = maximum operating temperature = 75°C

$V_{oc\_T1}$  = open circuit cell voltage at  $T_1$  = 21.7 V

$I_{sc\_T1}$  = short circuit current at  $T_1$  = 2.1 A

$I_{sc\_T2}$  = short circuit current at  $T_2$  = 2.4 A

$S$  = solar radiation in kW/m<sup>2</sup>

$I_{ph}$  = photo generated current

$I_s$  = cell saturation dark current

$E_g$  = Band gap energy of an electron

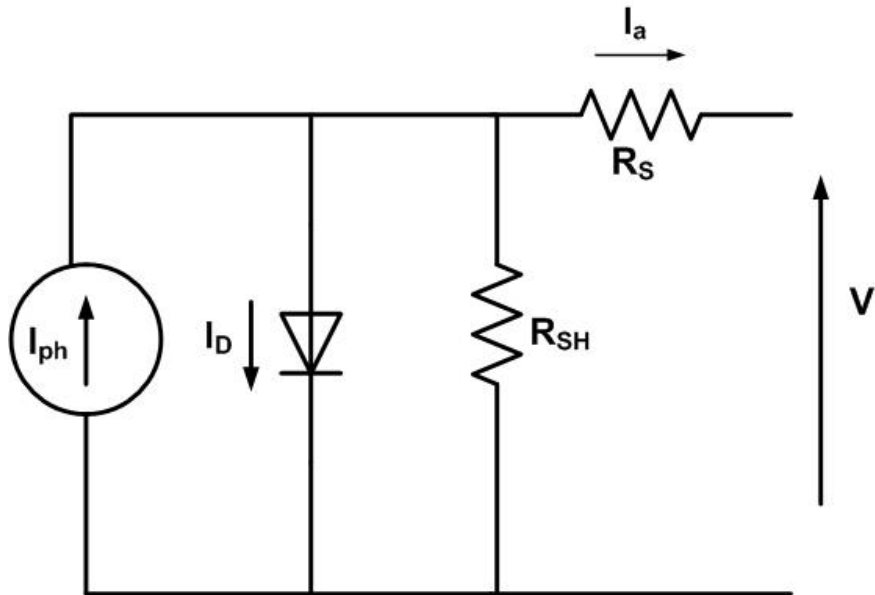


Fig. 3.1. Equivalent Circuit of a Solar Cell [9]

$V$  and  $I_a$  are the terminal voltage and current coming out of a solar module.

The relation between  $V$  and  $I_a$  is expressed as follows

$$I_a = I_{ph} - I_D - ((V + IR_s)/R_{sh})$$

where  $I_D$  is expressed as  $I_D = I_s[\exp(q(v+IR_s)/nkA) - 1]$ ;

$I_{ph}$  is given by  $I_{ph} = I_{ph\_T1} + K_i(T_{ak} - T_i)$  where  $I_{ph\_T1} = I_{SC\_T1} * S$ ;

$K_i$  is expressed as  $K_i = (I_{sc\_T2} - I_{sc\_T1})/(T_2 - T_1)$ ;

$I_s$  is expressed as  $I_s = I_{SC\_T1}(T_{ak}/T_1)^{3/n} \exp((qE_g/KA)((1/T_{ak}) - (1/T_1)))$ ;

$I_{s\_T1}$  is expressed as  $I_{s\_T1} = I_{SC\_T1}/(\exp(qV_{oc\_T1}/(nkT_1)) - 1)$

$R_{sh}$  = shunt equivalent resistance =  $\infty$

$R_s$  = series equivalent resistance

The V-I and P-V characteristics of the modeled solar array at various values of solar insulations are shown below from Fig. 3.2 to Fig. 3.5, where

$$V_{PV} = V \text{ and } I_{PV} = I_a [9]$$

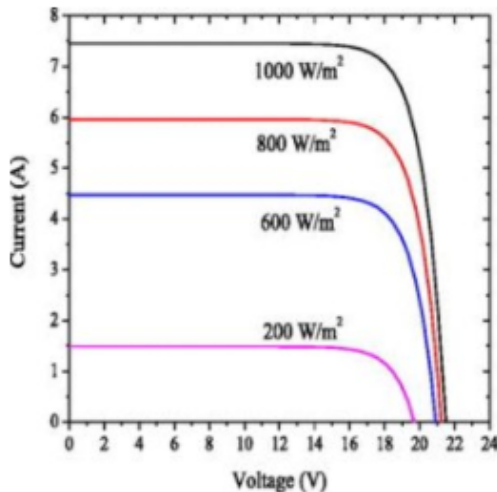


Fig. 3.2. I-V characteristics at different isolation levels [8]

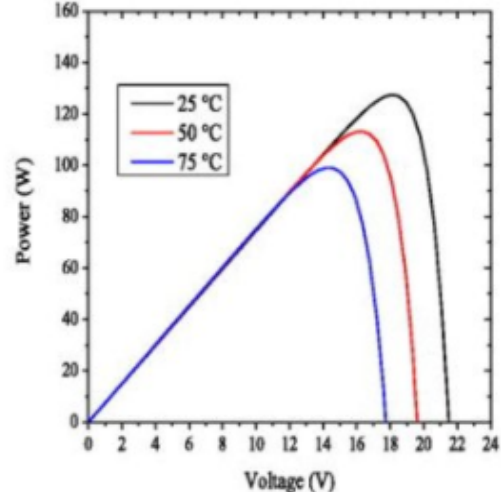


Fig. 3.3. P-V characteristics at different isolation levels [8]

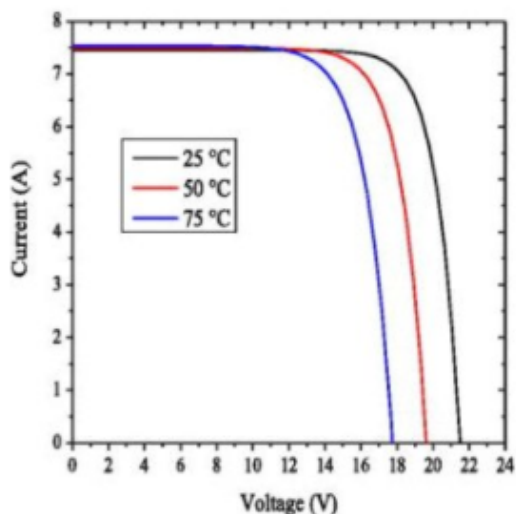


Fig. 3.4. I-V characteristics at different temperature values [8]

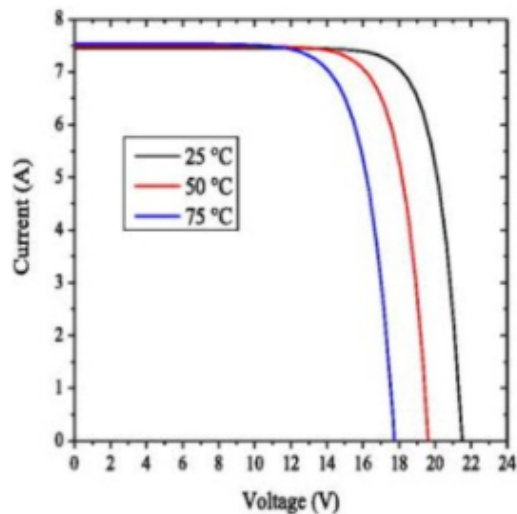


Fig. 3.5. P-V characteristics at different temperature values [8]

# Chapter 4 Hardware Development

A laboratory prototype of the proposed system consisting of a boost converter, bidirectional dc-dc converter, and sensors has been developed to validate the viability of the scheme. Implementation of hardware prototype requires selection of proper hardware components. Sizing and design issues about major components of the prototype are presented below.

## 4.1 Selection of Inductors

The choice of the inductor is influenced by current ripple allowance, switching frequency, operating voltage, and duty cycle. Since the primary side of half-bridge boost converters is a boost converter essentially, hence the inductance value can be found from the following expression,

$$L = \frac{DV_{pv}}{fs \Delta I}$$

Considering 20 kHz switching frequency, current limit to be 5% of PV operating current, PV MPP voltage of 17.5 V and current of 3.71 A, and Duty of 0.5 at MPP operation, we get an L value of 2.36 mH.

The inductor present in the bidirectional converter connected to the battery operates as an inductor of a boost converter while the battery is in discharging mode and operates as the inductor of a buck converter while the battery is in charging mode. Hence, the value of the inductor for a buck-boost converter can also be found out from the above equation. The battery current ripple is chosen fixed at 0.5A. To keep the frequency at 20 kHz with a battery voltage of 24V and to maintain the primary side DC-Link voltage around 34V, we get an L value of 1.2 mH.

The inductors considered are made of a ferrite core material with an operating frequency of 20 kHz approx.

## 4.2 Selection of Capacitors

The values of the capacitors chosen are based on the allowable voltage ripple and voltage that they have to withstand. Although the DC-Link capacitor maintains a voltage of 34V, the DC-Link capacitor can experience a maximum voltage of 45V. With a safety factor of 2, the voltage rating is chosen to be around 100V. To decide the capacitance value of the summing capacitor of the DC-Link, a high capacitance of 100  $\mu\text{F}$  is chosen to have a minimal ripple(less than 1%).

## 4.3 Selection of Switches

To determine the rating of the switches, on-state maximum current and off-state voltage are considered. For the boost converter switch(M1), the off-state voltage is around 34V. On-state peak current up to 4A, with a safety factor of 2 the minimum voltage and current ratings are chosen to be 68V and 8A.

For bi-directional converter switches(M2, M3), the maximum current can be around 4A and the off-state voltage is around 34V. With a safety factor of 2, the minimum voltage and current rating are chosen to be 68V, 8A.

All the three MOSFETS(M1, M2 & M3) are having a maximum of 72V and the current is 8A. IRF540 is a commonly available and cheap MOSFET whose specification matches our calculation (i.e Maximum voltage 100V, Maximum current 28A), hence we selected IRF540 as our switches.

## 4.4 Selection of Gate Drivers

We prefer to use isolated gate drivers as they provide isolation between the microcontroller and the main power circuit along with a simpler topology for high side control. For MOSFETs, with an operating frequency of 20kHZ, TOSHIBA photocoupler Drivers, isolated MOSFET driver TLP250 is found to be suitable. The

input side consists of a GaAlAs light-emitting diode. The output side gets a drive signal through an integrated photodetector. Therefore, the main feature is electrical isolation between low and high power circuits. It transfers electrical signals optically via light. The drivers have a maximum operating frequency of 25 kHz(>20 kHz) with  $\pm 1.5\text{A}$  of output current rating. [3]

## 4.5 PV Simulator, Battery, and Loads

PV panel output is realized using APLAB Technologies Solar Array Simulator SAS120/10 ODIV. The battery used is two 12 volts, 42 Ahr batteries from Quanta Amaron which is a Valve Regulated Lead Acid (VRLA) battery. Load is realized using rheostats.

## 4.6 Designing of Sensing Circuits

### 4.6.1 Voltage sensor

Three voltages measurements are required for working of the controller:

1. PV Array
2. Battery
3. DC-Link

Arduino ADC can measure voltage levels from 0-5V and map it to 0-1023 values. Hence we need to step down the voltages to this range for measurement. For this purpose, a voltage divider circuit was implemented with resistances in megaohms to reduce power wastage. The output from the voltage dividers was then fed into a buffer circuit made with Op-Amp 741 powered with a positive and negative 15V isolated power supply. The buffer circuit helps us minimize interstage loading. The buffer circuit is then followed by an RC circuit with an appropriate time constant to provide a smooth signal. Using hardware to smooth signals we reduced the computational effort required by the microcontroller.

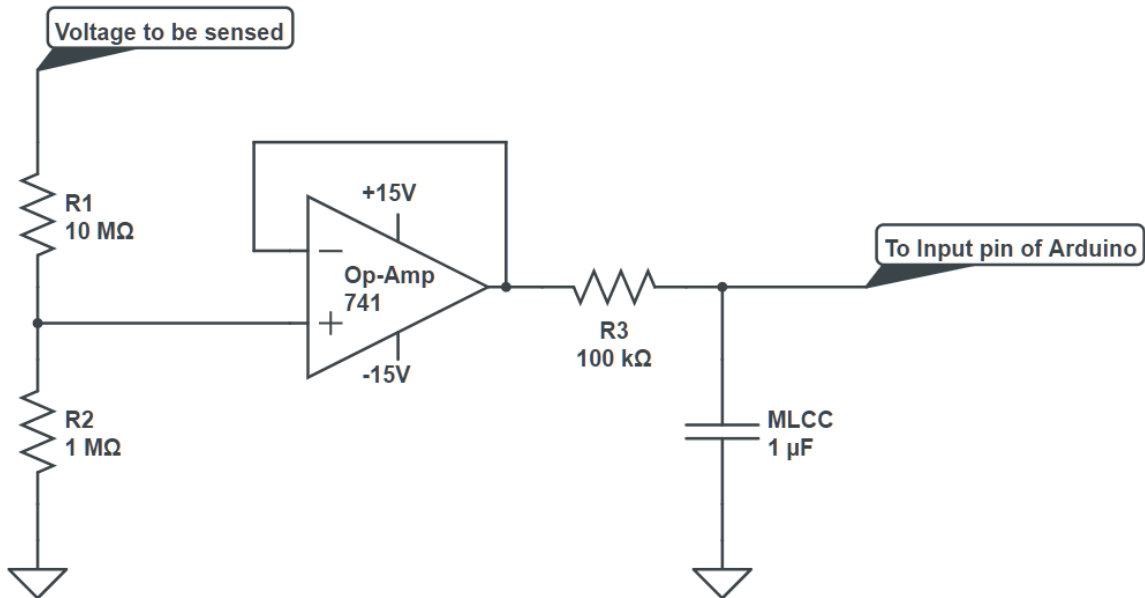


Fig.4.1. Schematic diagram of the Voltage sensor

The input from the sensor is further calibrated in the software.

Initially, we tried to power the 741 Op-Amp with just a +15V supply and grounded the -Vcc pin but this resulted in a floating output pin. Although a lot of articles suggest that it is a viable configuration, our Op-Amps required a -15V supply to -Vcc to give the intended output.

#### 4.6.2 Current sensor

Two current measurements are required for the working of the controller:

1. PV Array current
2. Battery current

We decided to use ACS712 as our current sensor IC. It outputs an analog output signal that varies with the bidirectional DC or AC current, sensed within the range -20A to +20A. The output is mapped between 0-5V. Since it is a hall effect

sensor it provides isolation between the high current circuit and the microcontroller. The IC can be powered by providing a single 5V supply. It is very reliable and low noise, thus very low computational effort is required.

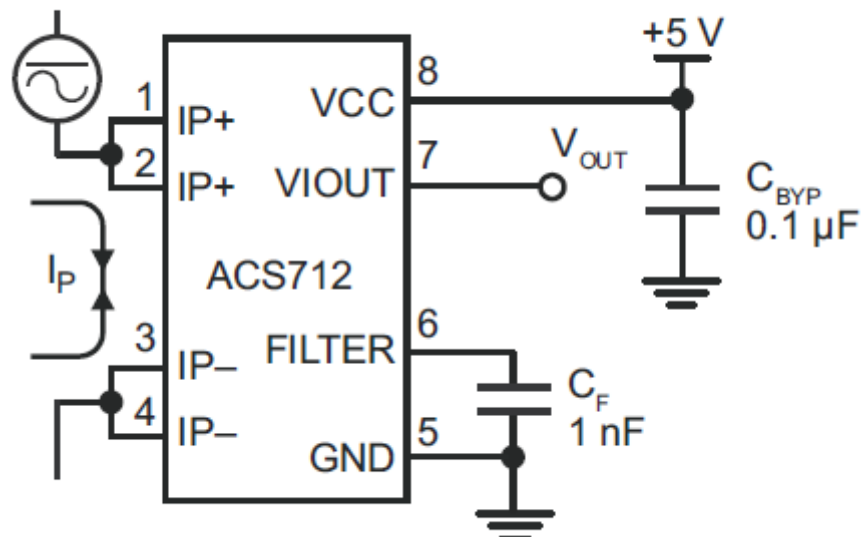


Fig.4.2. Schematic diagram of ACS712 [5]

## 4.7 Soft Starter Circuit

A soft start is required because of the high inrush current flowing when the batteries are connected to the main circuit. To prevent the inrush current, a delay circuit, which consists of two relays, a transistor, a capacitor, and a high watt resistor, is introduced. The circuit diagram is shown below:

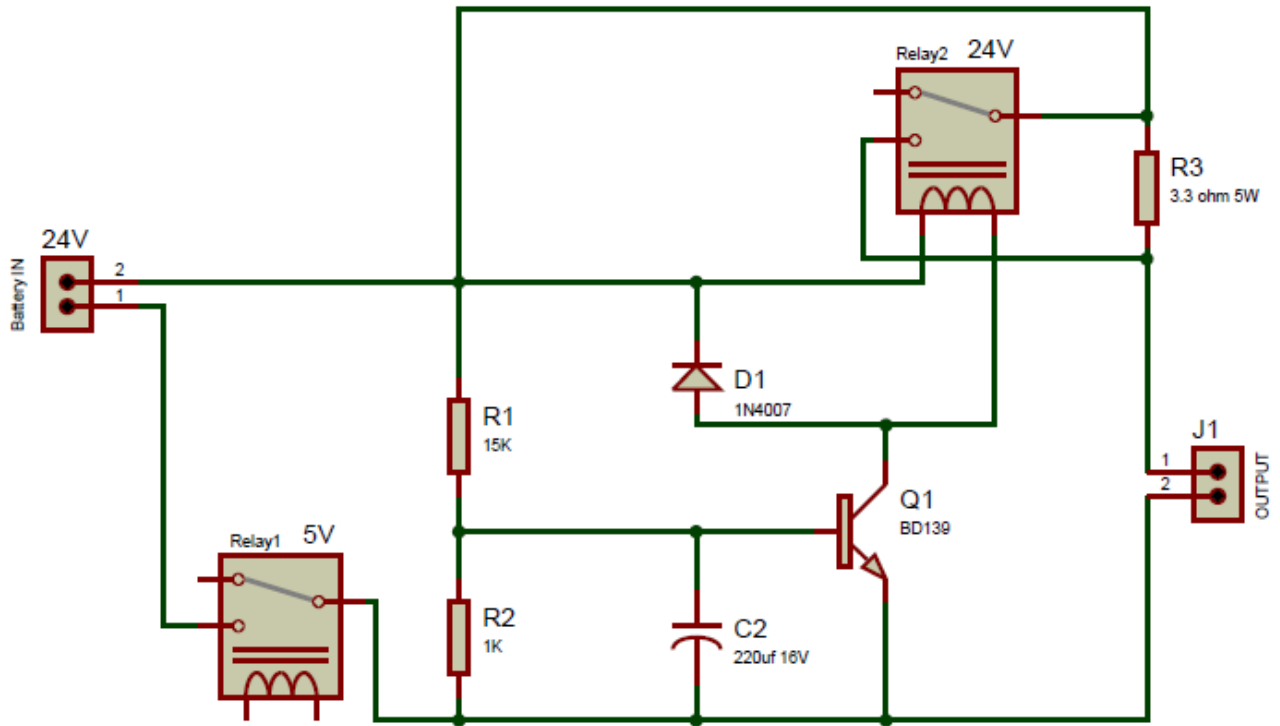


Fig. 4.3. Circuit diagram of Soft Start

Relay 1 is connected between the 24V Battery ground and the ground of the main circuit. When the Arduino gives a high signal, the Relay is triggered and the grounds of the battery and main circuit are connected.

R1, R2, and C2 make the delay network for the relay. R3 is the current limiting power resistor. Q1 is an NPN BD139 transistor to activate/deactivate Relay 2. D1 protects the Q1 from the relay's inductor's reverse currents. R3 is a 5W series resistor that limits the turn ON inrush current.

After Relay R1 is triggered the capacitor C2 starts charging with the time constant  $R2 \cdot C2$ . 24V battery is connected to the main circuit through R3. When the capacitor is sufficiently charged, Q1 switches ON. This flow of current through Q1 triggers Relay 2. The resistor R3 is bypassed and the 24V battery is directly connected to the main circuit. The value of the R3 has been set to 10 ohms.

## 4.8 Relay selection

Two relays are used in the soft starter circuit. The first relay is required to connect the ground of the battery to the main circuit so it is triggered by the Arduino itself hence the desired relay voltage is 5V(Voltage across relay coil) while another relay is going to be connected directly with the battery voltage after a delay of 220ms(after the relay1 is triggered) hence the relay2 voltage is 24 V.

## 4.9 Fuse Selection

Properly selected fuses prevent accidents by breaking abnormal currents when they flow through electric circuits. The value of the fuse should be such that the current rating of the fuse is equal to the maximum allowable current + 1. In our case maximum allowable current throughout the circuit is 4A, so a fuse of 5A current rating is selected which is available in the lab.

## 4.10 Hardware Prototype Photos

Various pictures depicting the hardware prototype developed are shown in Pictures for the hardware prototype developed, are shown in Fig. 4.4

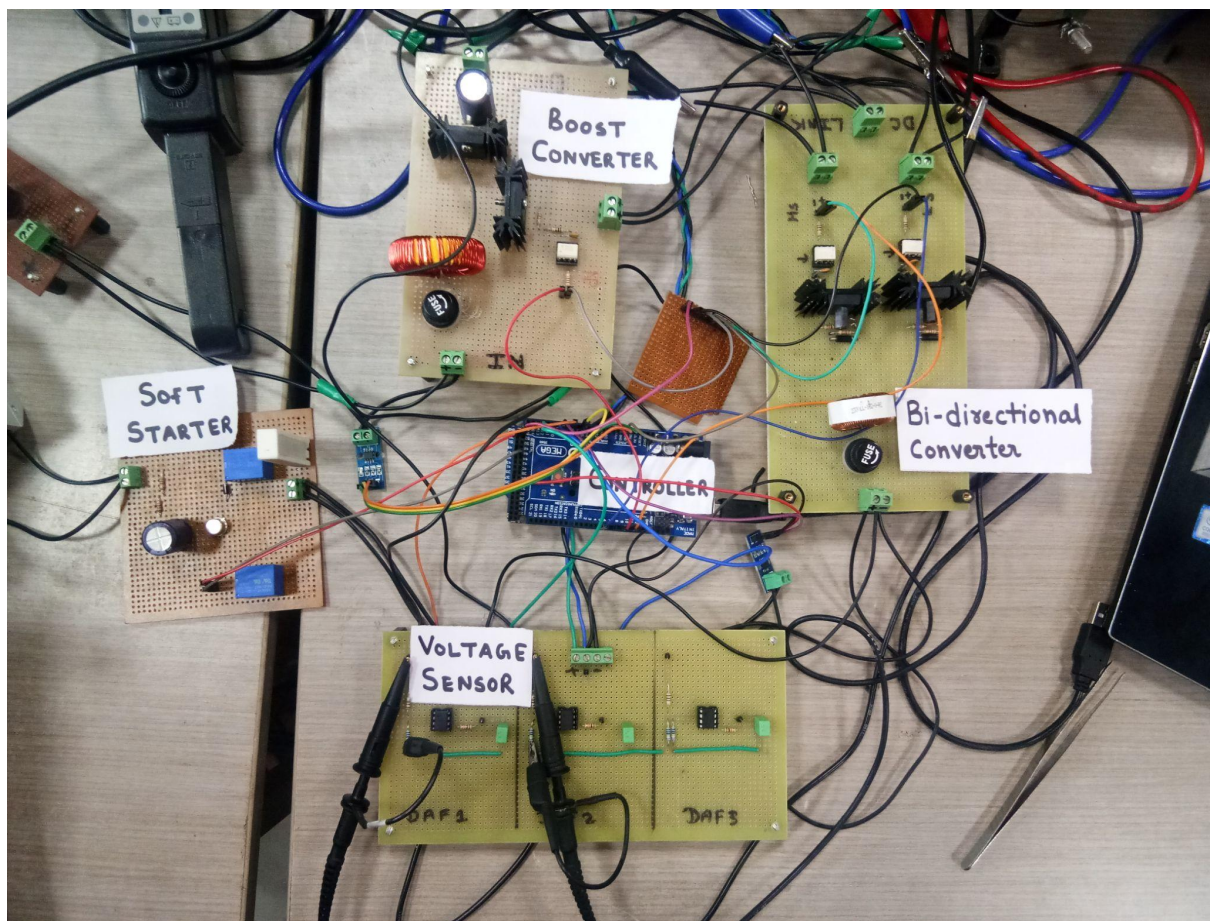


Fig. 4.4. Complete Circuit

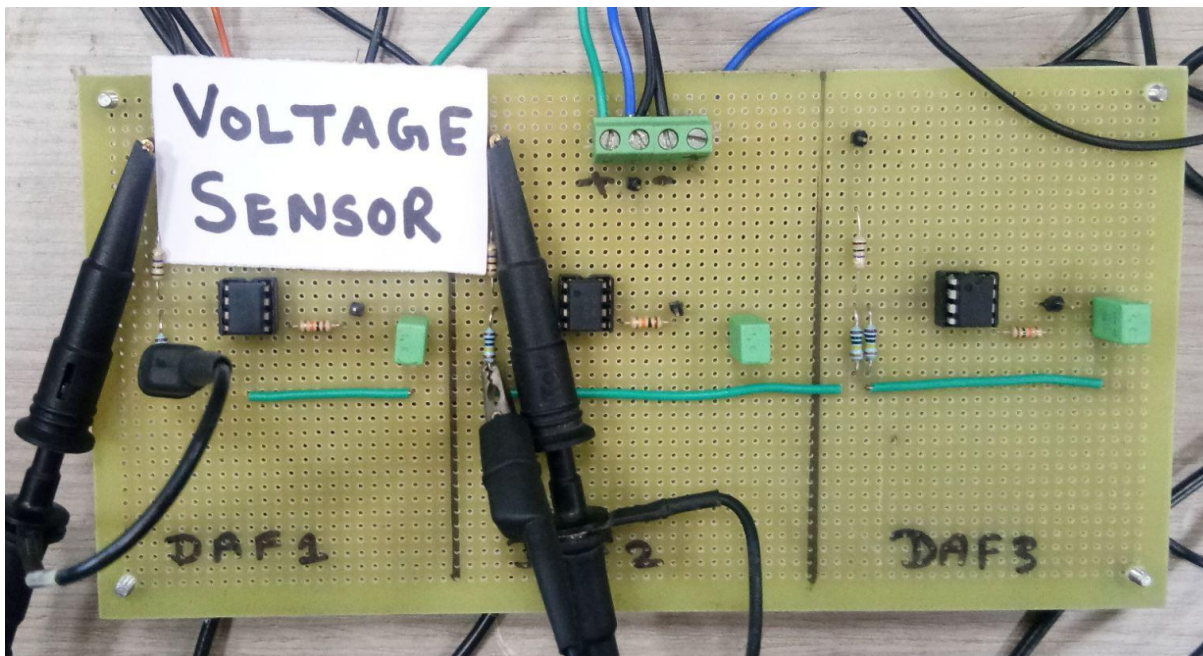


Fig. 4.5. Voltage Sensor

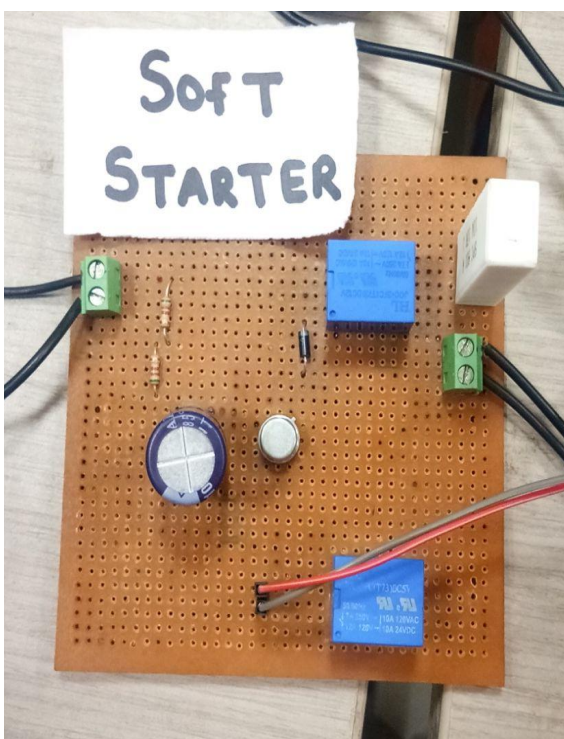


Fig. 4.7. Soft Starter

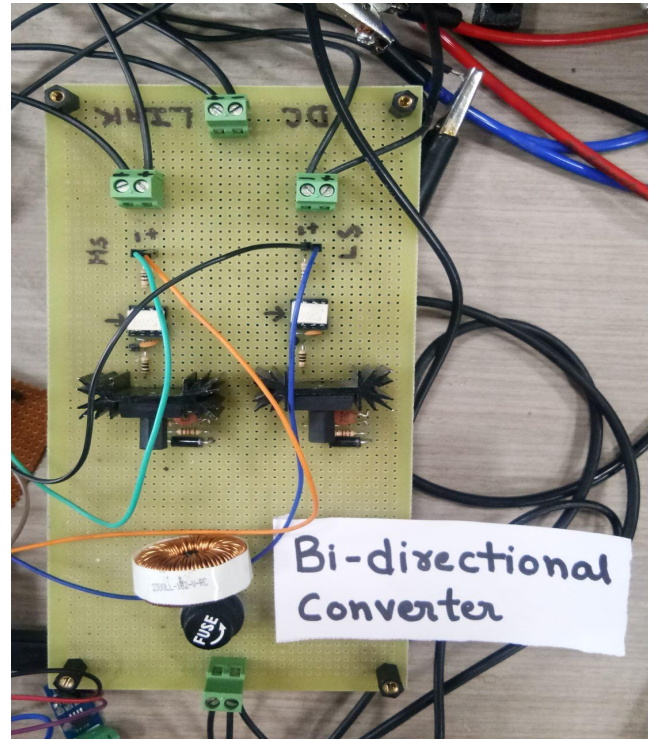


Fig. 4.8. Bi-directional Converter



Fig. 4.6. Complete Setup

# Chapter 5 Control Scheme and Software

## 5.1 Modes of Operation

The boost converter and the bi-directional converter operate in harmony so that the output DC-Link voltage remains stable at the set reference point. It is ensured that the excess energy from the solar panels is transferred to the battery if the battery is not fully charged.

Broadly speaking there are two modes of operation:

1. Maximum Power Point Tracking (MPPT) mode
2. non-MPPT mode

### 5.1.1 MPPT Mode

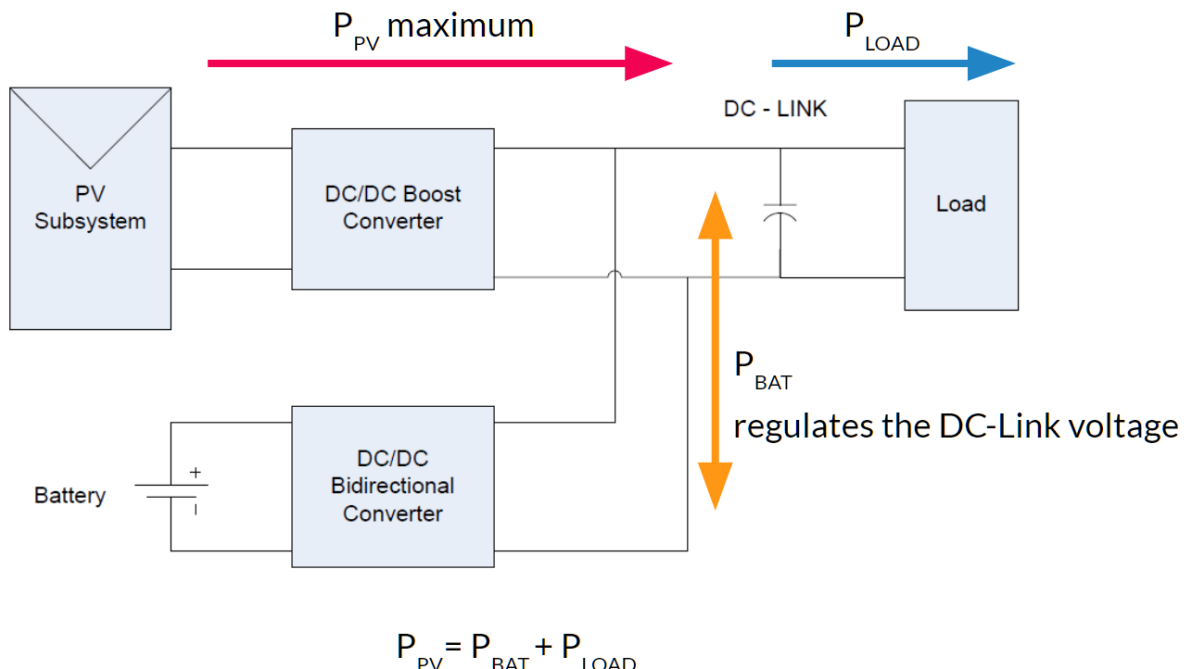


Fig. 5.1.1.1 Power Flow in MPPT Mode

In MPPT mode, maximum power is being extracted from the PV array. Depending on the load requirement, the bidirectional converter will charge or discharge to absorb or provide power. If the power equation is balanced then the DC-Link voltage will be at the reference voltage. Thus the bidirectional converter strives to keep the DC-Link voltage at the reference level.

### 5.1.2 Battery-Only (BO) Mode

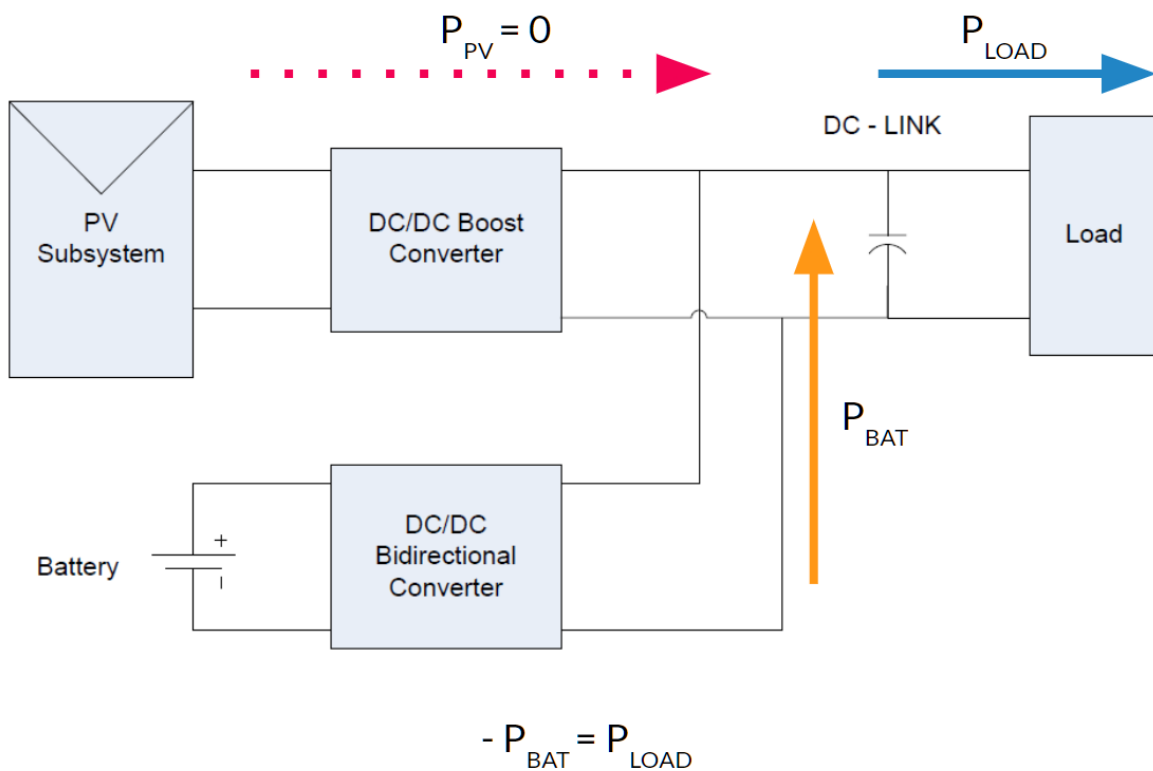


Fig. 5.1.2.1 Power Flow in BO mode

Battery-Only Mode is MPPT mode in disguise. The only difference here is that the power from the PV array is zero. Thus the bidirectional in the pursuit to keep the DC-Link voltage at the reference voltage will provide the power.

### 5.1.3 Non-MPPT Mode

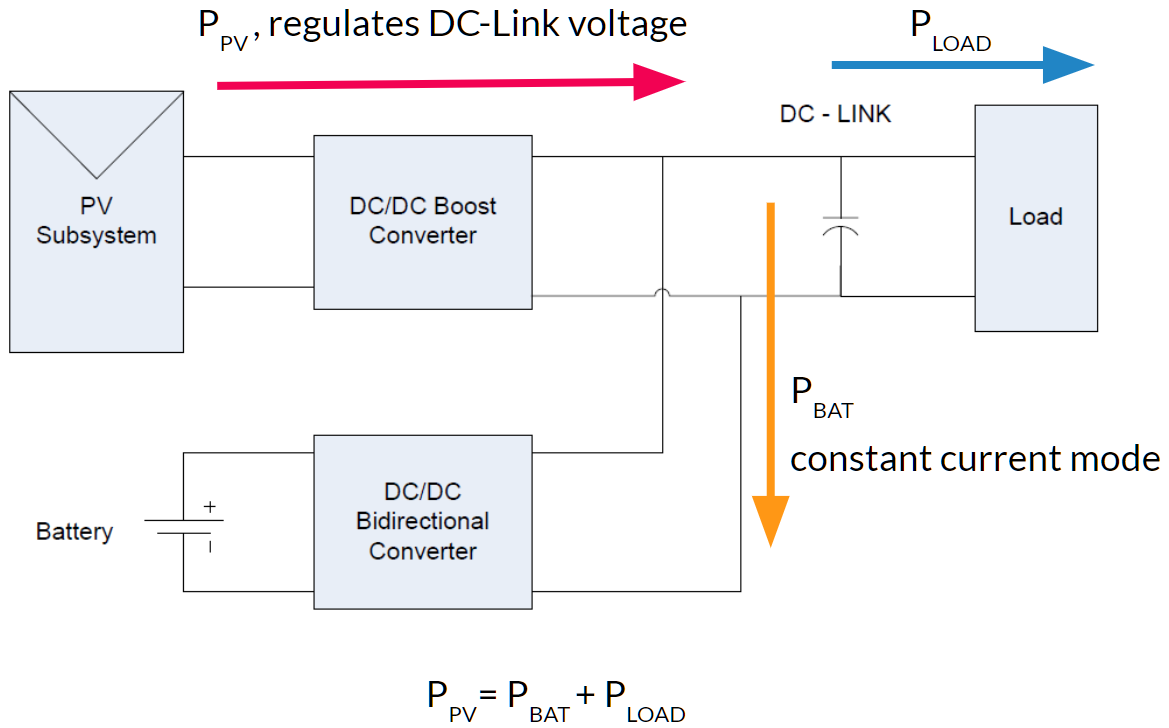


Fig. 5.1.3.1 Power Flow in non-MPPT mode

If in the MPPT mode, the PV array is producing so much power that the battery and load are unable to absorb then the controller will switch the mode to non-MPPT. In this mode, the charging current is kept constant implying that the  $P_{BAT}$  will be constant and positive. The boost takes on the responsibility of balancing the power equation by regulating the DC-Link voltage.

If a power deficit is observed in the load or the battery then the controller will again switch the mode back to the MPPT mode. In MPPT mode the constant charging current restriction is removed and the PV array will provide as much power as it can.

## 5.2 MPPT Algorithm: Perturb and Observe (P&O)

We choose Perturb and Observe (P&O) as our MPPT algorithm because of the following factors. We used cheap voltage sensors and current sensors which did not provide very precise data which is essential to keep other MPPT algorithms, like incremental inductance, stable but P&O is very robust and can work very well with noisy data. Secondly, P&O does not require any sophisticated computations and thus was well supported by our microcontroller.

Working of the algorithm: At every point of operation the duty cycle is varied slightly (perturbed) in a chosen direction and the output power is observed. If the observed output power is greater than what it was previously observed we continue to perturb the duty cycle in the same direction. In the case that the power observed was less than it previously observed then the direction in which perturbation is being done is reversed.

When maximum power is reached, the P&O algorithm keeps oscillating between the maximum and its 2 neighboring operating points.

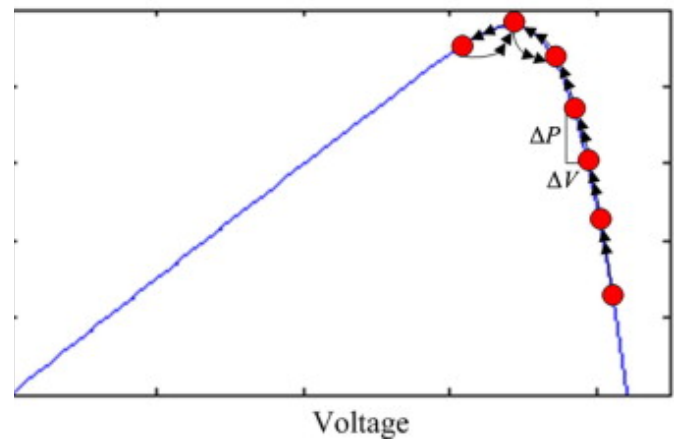
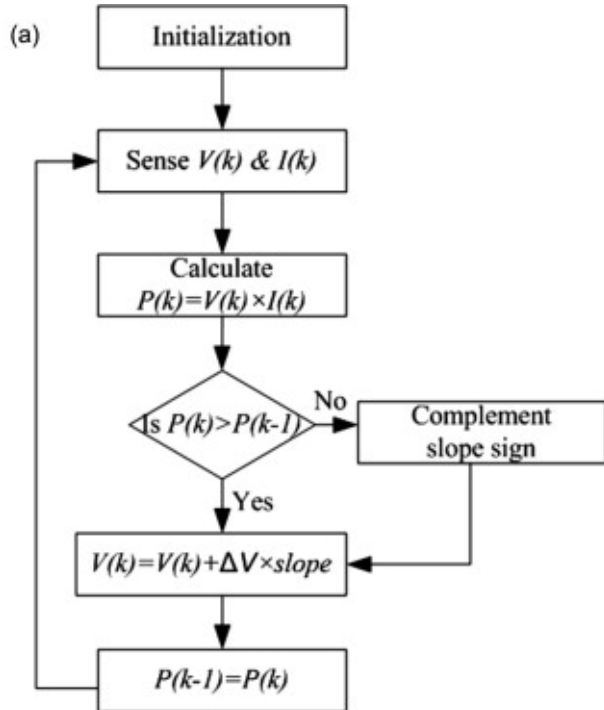


Fig. 5.2.b Power-Voltage hill climb representation in P&O algorithm [4]

Fig. 5.2.a Block control system diagram of P&O mode [4]

## 5.3 Control System

### 5.3.1 Duty Cycle Control System:

The control systems implemented to calculate the duty cycles for the high-side of the bidirectional converter and boost converter are demonstrated below. The basic structure has been borrowed from Chakraborty, Suvamit, and Amod C Umarikar. "Standalone PV system based on Isolated Quasi Z-Source Converter." 2018 IEEE International Conference on Power Electronics, Drives and Energy Systems (PEDES). IEEE, 2018. [6]

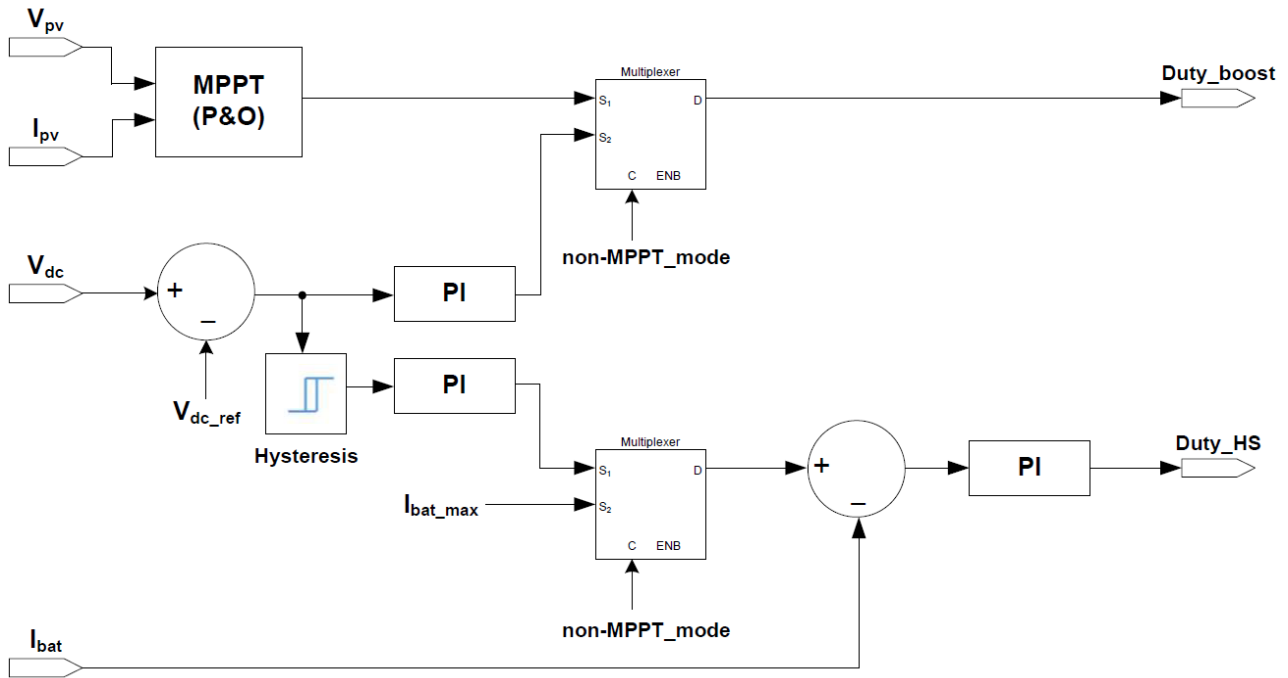


Fig. 5.3.1.1 Control system block diagram for boost and high side duty cycle

Duty of LS is made to follow Duty HS through a linear fashion by incrementing with a constant. The dead band is ensured before the duty cycles are updated to the timers. If Duty HS decreases rapidly, a dead band is forced and duty LS is adjusted. Thus a small jerk can be observed in the results in such a case.

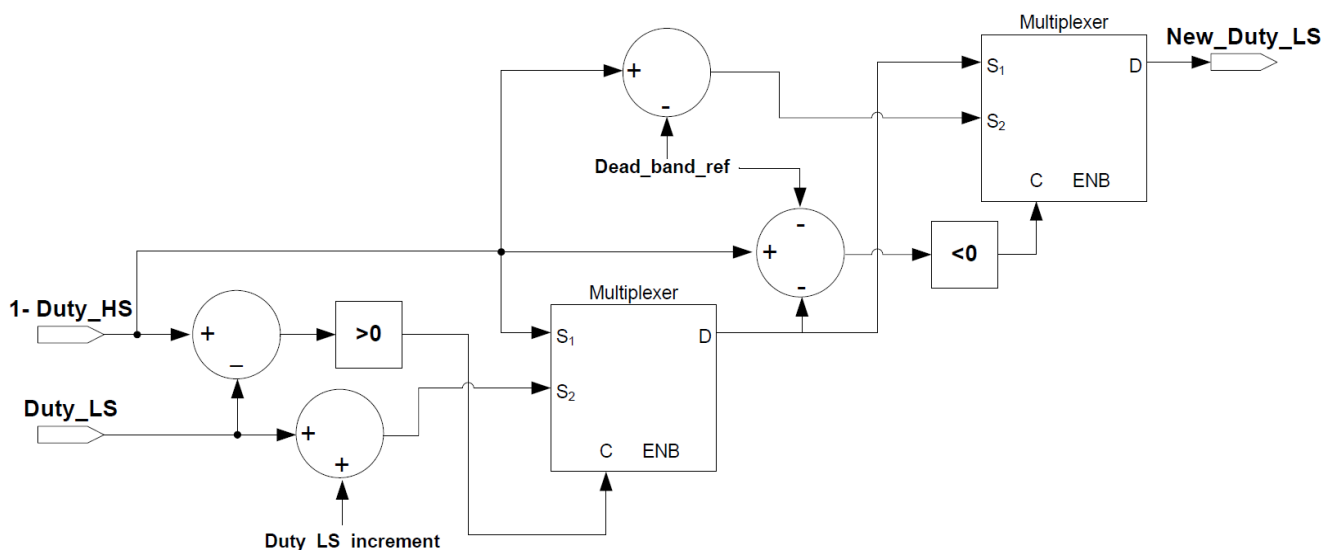


Fig. 5.3.1.2 Control system block diagram for low side duty cycle

### 5.3.2 Mode Selector System:

A control system is required to continuously monitor the current state of the system. If some parameter indicates power excess or deficit then the mode of the system needs to change accordingly.

As we developed our software and hardware together a mode change system was developed impromptu during the hardware development phase of the system. An attempt has been made to explain its workings.

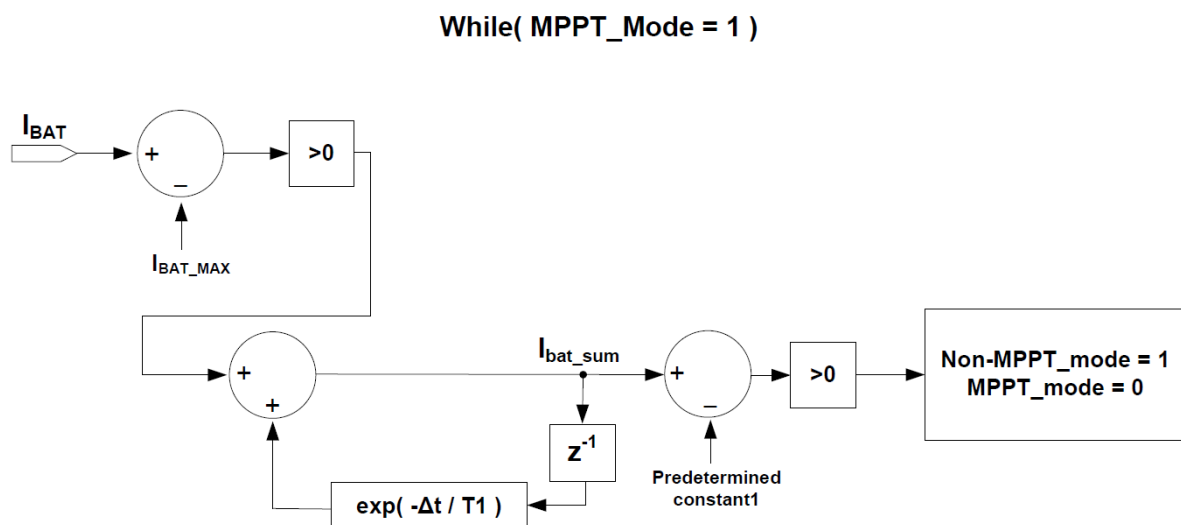


Fig. 5.3.2.3 Control system block diagram for Mode Selector in MPPT Mode

While the system is in MPPT Mode, the battery current is observed and it is checked for exceeding the maximum current. Whenever it is high, a signal ‘1’ is passed to the exponential summer with a known time constant. Based on this time constant a constant is determined. This system is used to check for over-current. If the over-current is detected then the non-MPPT mode is engaged.

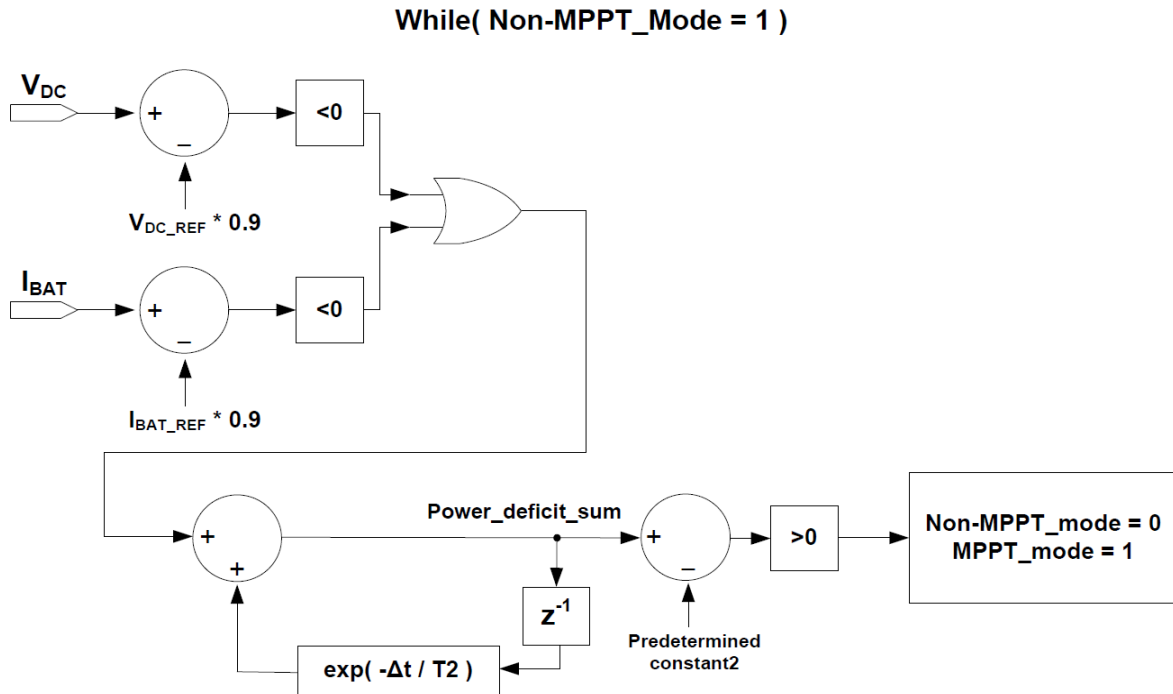


Fig. 5.3.2.4 Control system block diagram for Mode Selector in non-MPPT Mode

Similarly, when the system is in the non-MPPT mode it is observed for power deficit by using the voltage at DC-Link and the charging current. If any of these are below the threshold values, a ‘1’ is fed to the exponential moving average. If the sum crosses the predetermined constant calculated from the time constant then the system is transferred to the MPPT mode.

## 5.4 Overview of Software Development

We used the Arduino Mega 2560 as the development board for this project to speed up the development process. The major advantages of using the Arduino Mega are its simplified build environment and easy debugging tools. Git version control was used during the development phase.

The disadvantages of using the Arduino were the lack of short circuit detection which is available in higher-end digital signal processors (DSP), lack of inbuilt features such as complementary PWM with a dead zone, sampling of sensor data cannot be done at a fixed frequency and independently of the main code loop.

We build custom functions to produce the required Complementary PWM set 20 kilohertz with the dead band. To set the PWM 20 kilohertz the datasheet of the ATmega2560 was referred and the control registers of the timers were manipulated. We used RC circuits to smooth the sensor data instead of relying on software smoothing which requires additional computation and also cannot be done very effectively in Arduino due to its lack of sampling.

Initially, we tried to implement a soft start with just software but It was not always reliable. Thus, we had to build a hardware soft start relay mechanism.

## 5.5 Working of the Code

Every arduino code has 2 predefined functions: `setup()` and `loop()`.

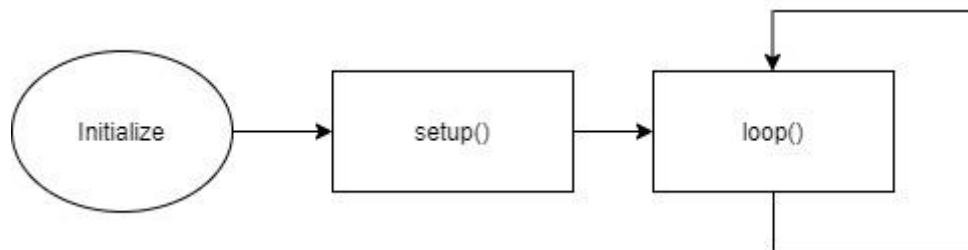


Fig. 5.5.1 Block diagram of basic code structure in Arduino

In the initialization stage, global variables are allocated. We shall discuss what are the global variables used in our code later.

The `setup()` function is executed once. It is responsible for `pinMode` selection, Serial monitor initialization (for debugging), and timer configuration for PWM pins.

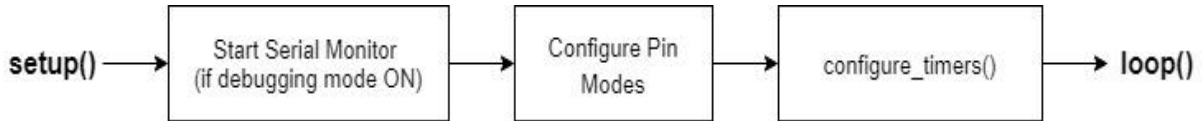


Fig. 5.5.2 Block diagram of `setup()`

The `loop()` function executes after the `setup()` finishes. It keeps returning to itself. Several other functions are called in the loop to serve as the main logic of our controller.

### 5.5.1 Global Variables

Declaration of pins

Debug mode, relay ON time, DC-link voltage reference

Present duty cycles of HS, LS

LS Duty cycle delta and Dead Bandwidth

PI of  $I_{bat\_ref}$  generator

PI of non-MPPT mode

Soft start  $k_p$ ,  $k_i$  for hs

Post soft start  $k_i$ ,  $k_p$  for hs

Soft start mode, current relay state

MPPT (P&O) mode config variables

Current and Voltage readings and reference variables

### 5.5.2 User-defined Functions

`configure_timers()`: Three PWM pins are required for the functioning of the controller. Each pin is controlled by a separate timer in the microcontroller so that we can control both the frequency and duty cycle. These have been configured to 20kHz each and synchronized.

`update_timers()`: The updated duty cycle variables are assigned to the timer registers.

`take_inputs()`: `analogRead()` is used to take input from the pins. This data with noise is smoothed by taking a simple average and then assigned to the corresponding voltage or current reading variables.

`calc_iref()`: A PI with input parameters DC-Link voltage reading and reference is used to set the reference battery current.

`calc_and_limit_duty_hs()`: A PI with input parameters battery current reading and reference is used to calculate the duty of high side MOSFET. The duty cycle is ensured to be within safe bounds.

`calc_and_limit_duty_ls()`: Duty LS is made to follow Duty HS linearly using a fixed delta step. Dead band is ensured. Bound on duty LS is applied for safety.

`ensure_dead_band()`: Additional check to ensure deadband.

`mppt_func()`: Perturb and Observe (P&O) algorithm is implemented and the duty cycle variable of boost is updated.

`non_mppt_func()`: A PI with input parameters reading and reference of DC-Link voltage is used to calculate the duty cycle of boost.

`soft_start()`: Switch relay ON after specified `relay_on_time`. Set `kp`, `ki` for duty HS to post `kp`, `ki` config after the set time interval from the soft start.

mppt\_mode\_selector():

In MPPT Mode: If there is power excess, battery charging current is above the threshold, then switch to Non-MPPT mode.

In non-MPPT Mode: If there is power deficit, observed from lower than required DC-Link voltage, then switch to MPPT Mode.

serial\_print(): Print required values of variables for debugging.

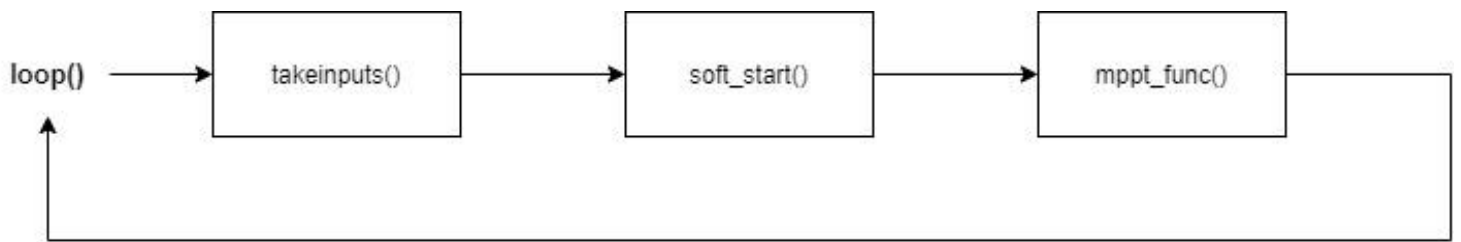


Fig. 5.5.3 Block Diagram of Loop before Relay is turn ON (Pre Soft-Start)

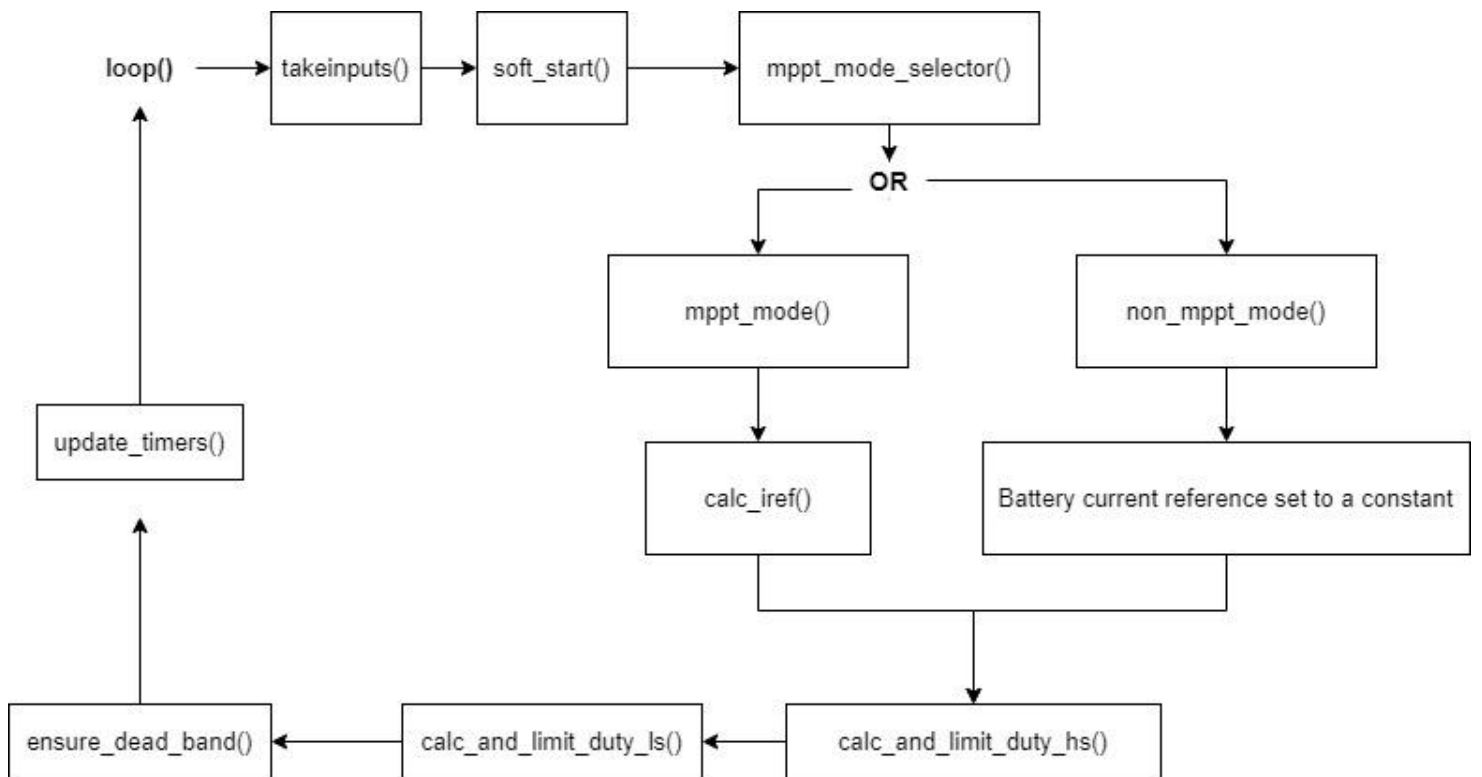


Fig. 5.5.4 Block Diagram of Loop after Relay is switched ON (Soft-Start Mode)

After a few seconds, `soft_start()` replaces `kp, ki` of HS duty cycle with post soft start configuration, and the function is taken out of the loop and soft start is complete

# Chapter 6 PCB Design

We applied design for assembly principles while designing the PCB. The crux of this approach is to design in such a manner that the ease of assembly is maximized. This approach is known to decrease the time required for completion of the project, reduces the risks involved, and results in fewer revisions which lower cost and saves time. [7]

We referred to the datasheets of the components and also in some cases took the effort to measure the component dimensions ourselves. The following were the key points of consideration in the design process:

<b>Layout</b>	Pad Size and Shape Hole Size Package Size Board Size and Shape Component-to-Component Spacing Component-to-Edge Spacing Componnet-to-Hole Spacing Orientation Via in Pad
<b>Assembly</b>	Requirements Wire harnesses Coatings Wire bonding Mechanical Components Thermal Relief EnclosureSize and Shape
<b>Production</b>	Reflow soldering Wave Soldering
<b>Testing</b>	Electrical Functional Circuit Testing
<b>Standards or Certifications</b>	Bill of Materials Gerber Files Assembly drawings IPC, SMTA, ISO

Fig. 6.1 Key points of consideration in PCB Design [7]

The electronic computer-aided design (ECAD) software we used was Proteus. The frontside, backside, and layout of the PCB are shown in fig. 6.2, 6.3, 6.4 below:

Due to lack of time, we were only able to complete the layout phase.

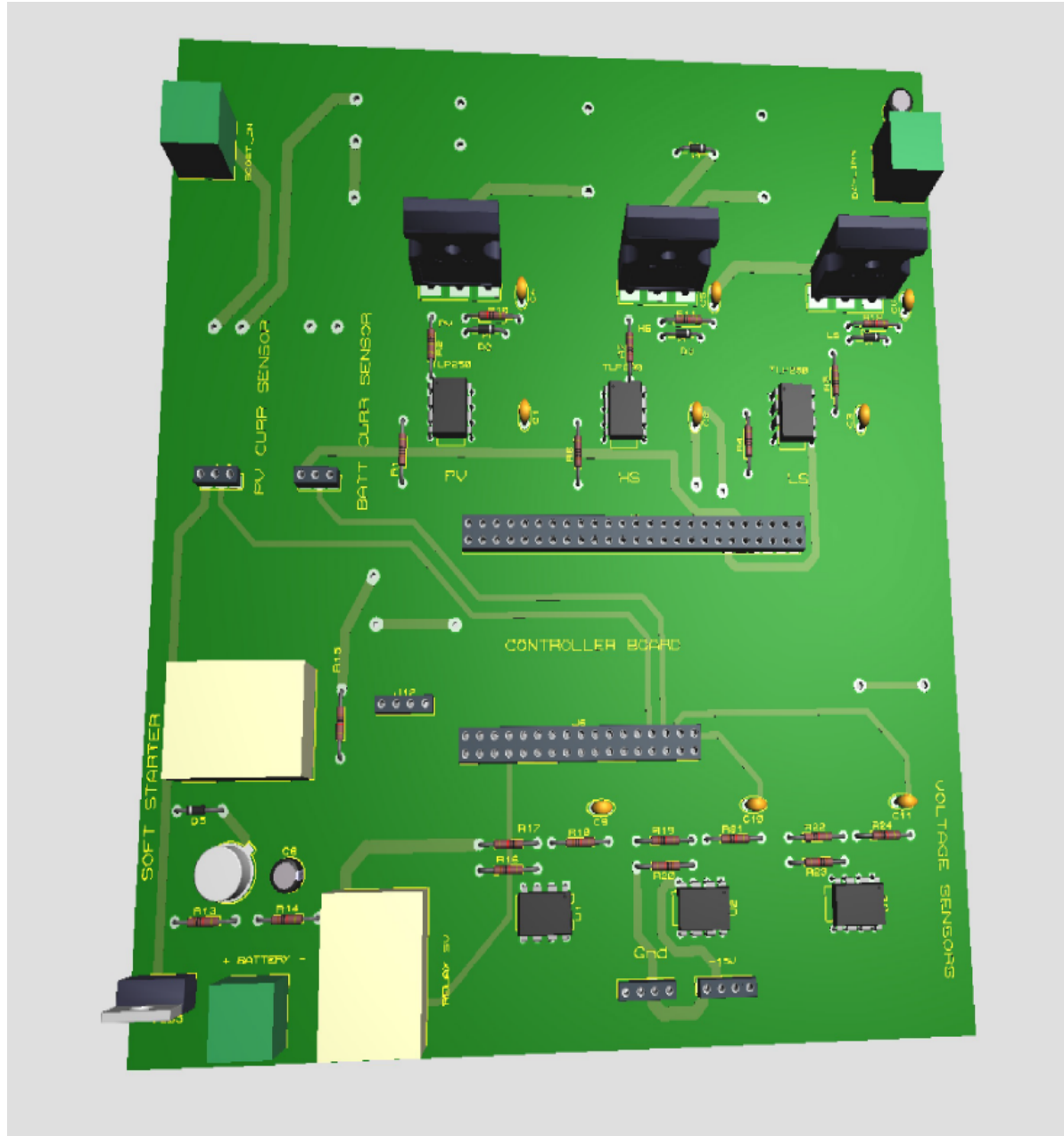


Fig. 6.2. PCB FrontSide

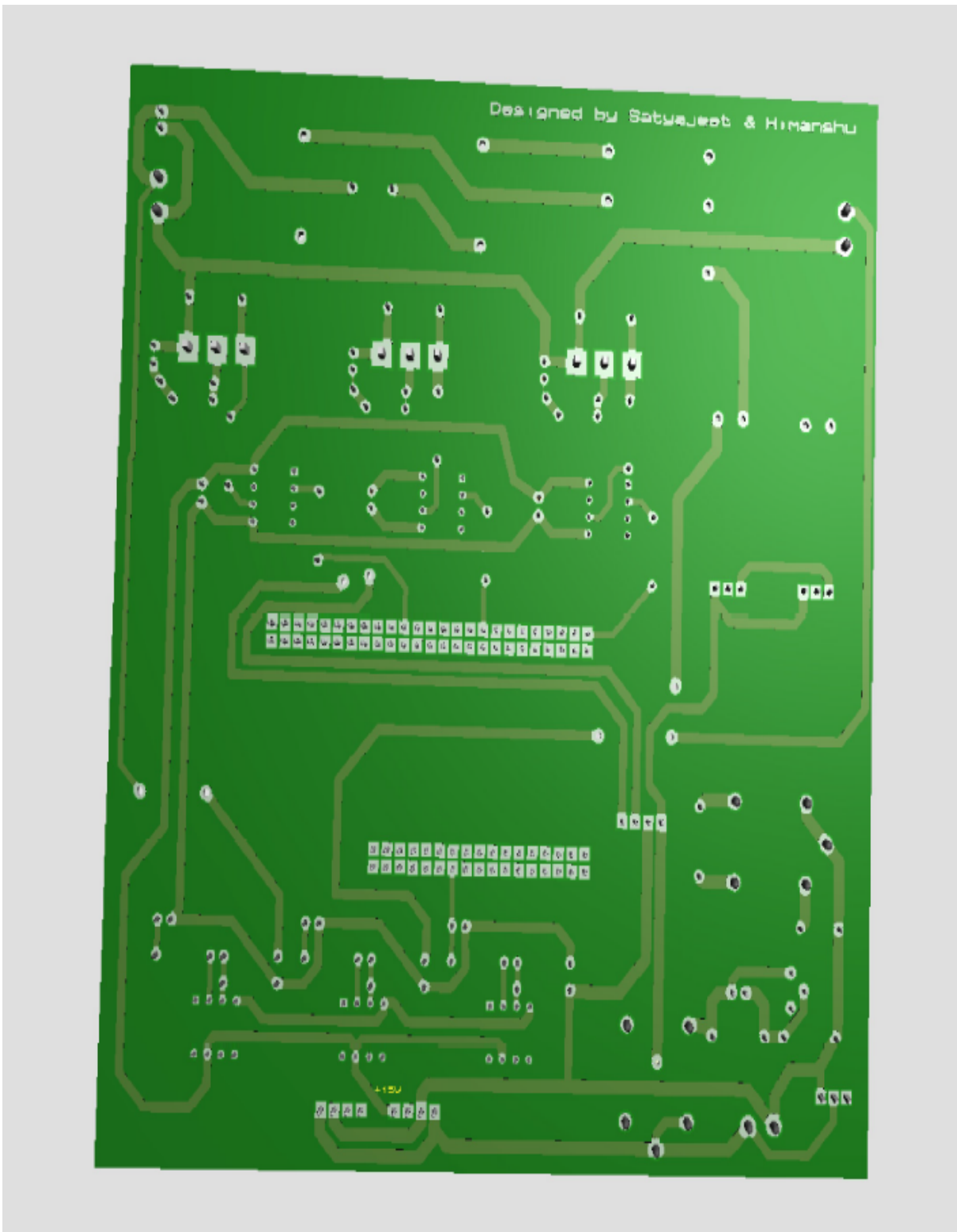


Fig. 6.3. PCB Back Side

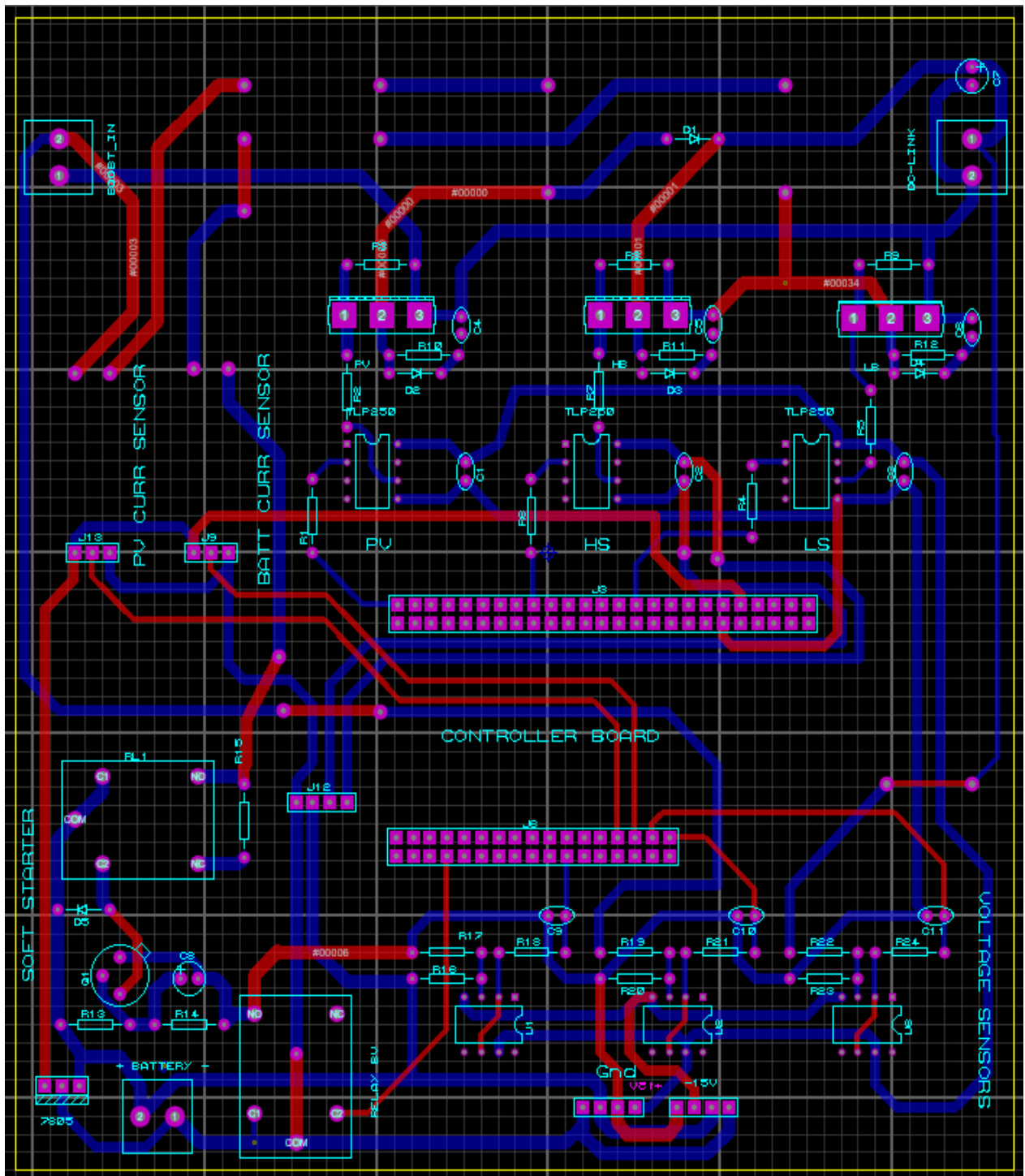


Fig. 6.4 PCB Footprint

# Chapter 7 Results

## 7.1 Experimental results

### 7.1.A Battery-Only (BO) mode

When the PV array is not connected to the system or is not providing any power, like during the night, then the system is running in Battery-Only (BO) mode.

Here is a full scope reading when the system is started in BO mode.

A load of 20W is set. DC-Link voltage reference being 34V and the battery voltage is 24V.

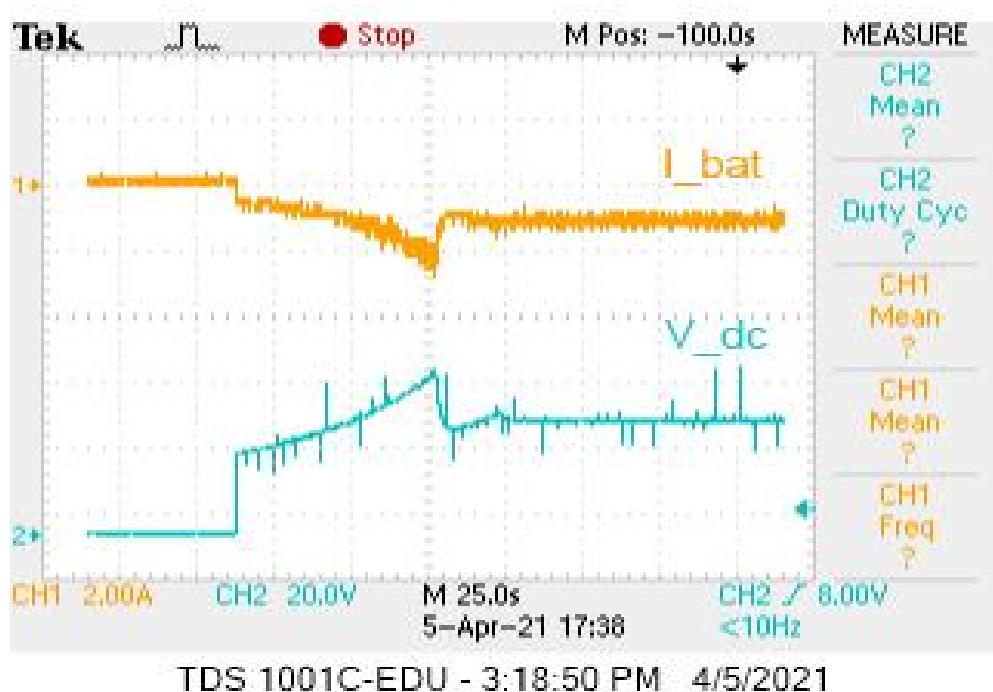


Fig. 7.1.A.1 Full waveform in BO mode

As we have implemented a soft starter, no spike is observed during the starting.

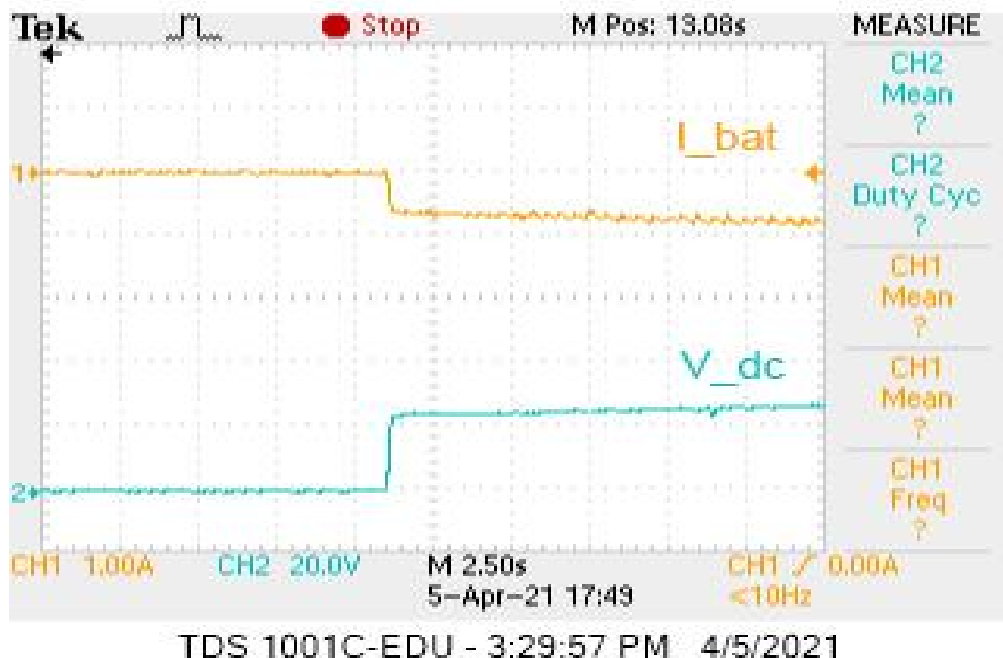


Fig. 7.1.A.2 Soft start waveform in BO mode

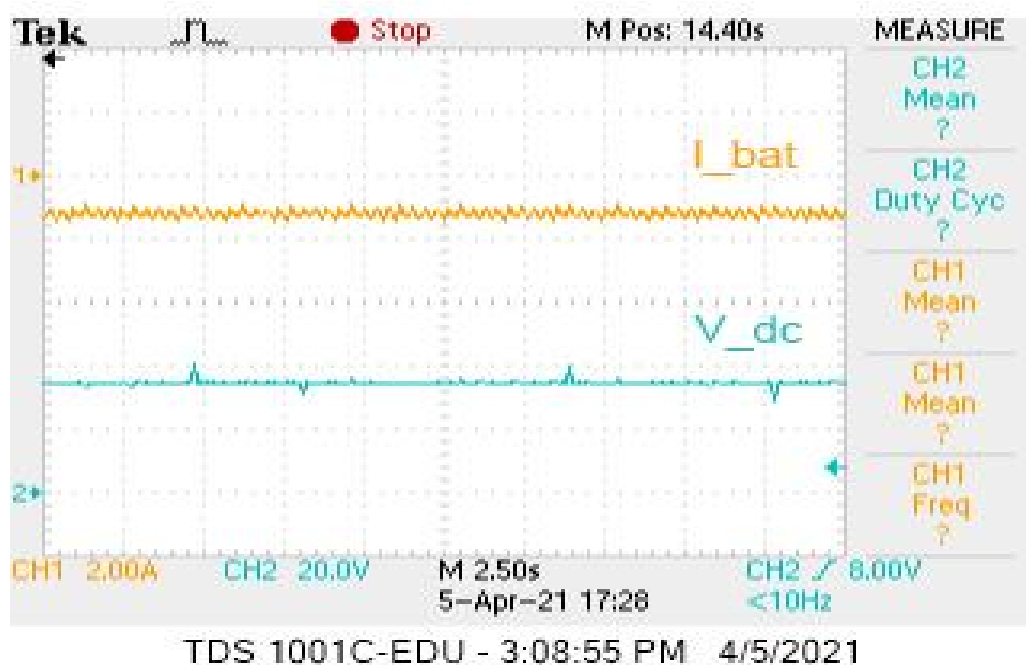


Fig. 7.1.A.3 Steady State waveform in BO mode

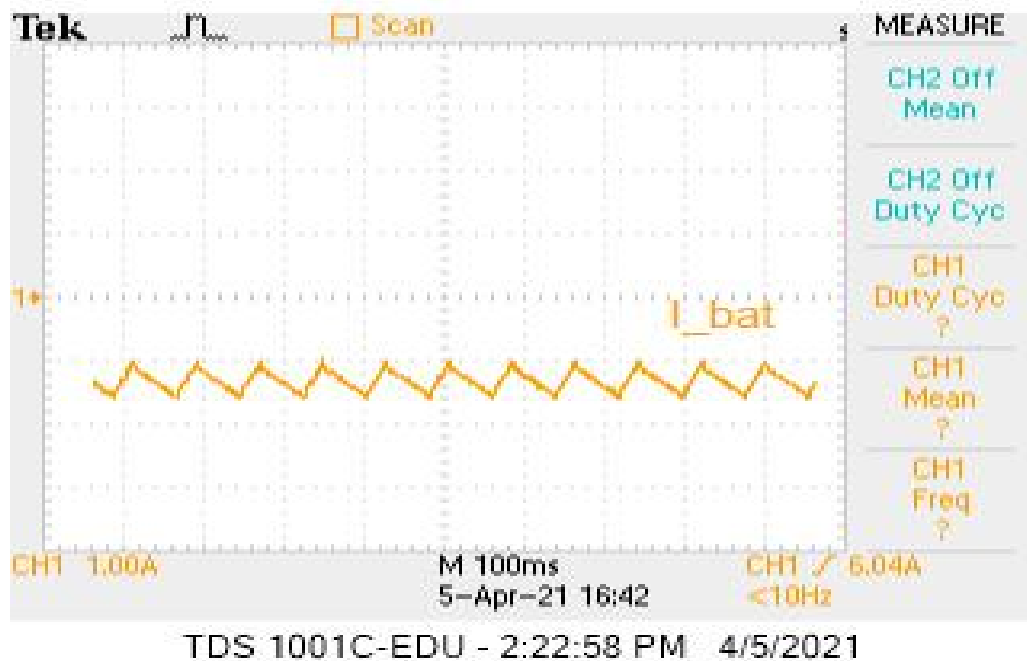


Fig. 7.1.A.4 Steady State Current Ripple in BO mode

### 7.1.B MPPT Mode

In MPP mode, the PV array provides a power of 64W. If the load requirement is less, then excess power is used to charge the battery. Else the battery provides the power deficit.

Here, the load is changed from 30W to 70W.

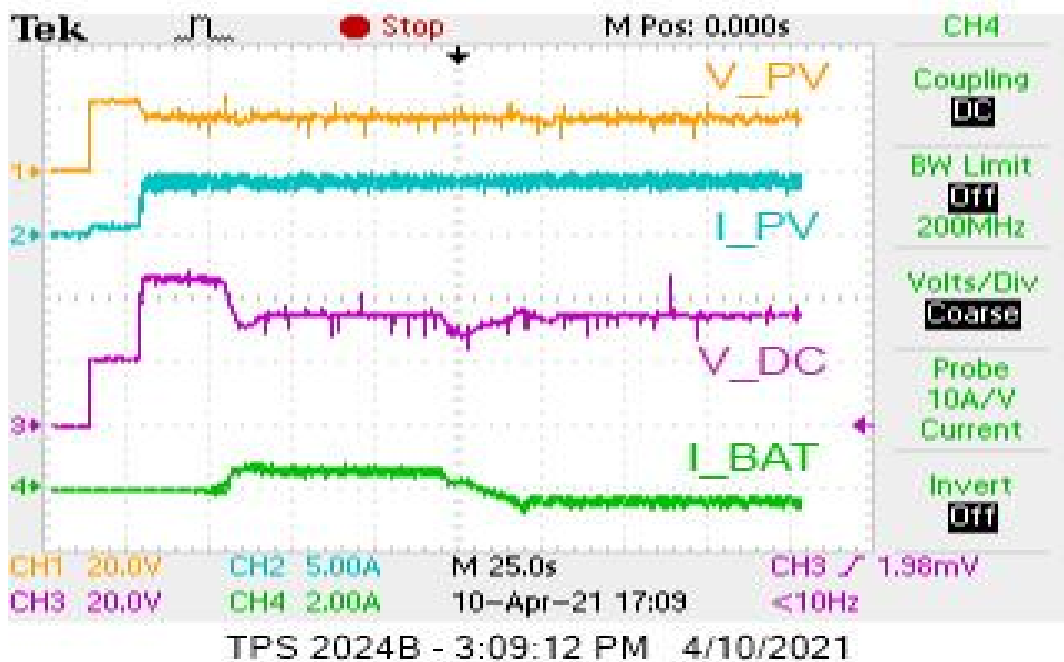


Fig. 7.1.B.1 Full waveform for Charging to Discharging of battery in MPPT Mode on load change.

Here is an example of how the system reacts when the PV module is initially running in BO mode. Then the PV array starts giving power as the irradiation is back. Then the PV array again stops working when irradiation is gone.

Thus the system moves from BO to MPPT to BO.

The transition is smooth and the control system is able to maintain the DC-Link voltage as required. The load remained constant at 30W.

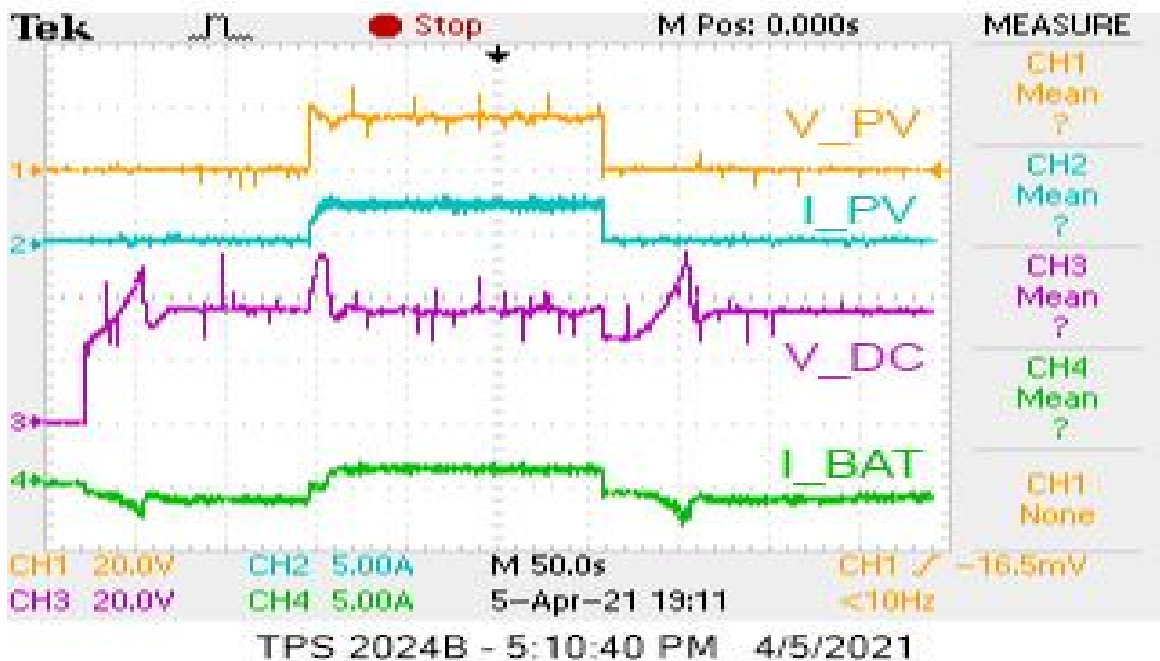


Fig. 7.1.B.2 Full waveform for mode switching from BO to MPPT to BO

### 7.1.C NON-MPPT Mode

Initially, the system is in MPPT mode. The load is set at 30W. The excess power from the PV array is being used to charge the battery.

Then at (1) the load was reduced to 15W. The non-MPPT mode is triggered as the voltage of the DC-Link spiked over the threshold voltage. It could have also triggered due to over current but here the voltage spike is observed. Thus at (1) mode change is observed.

The controller is set to keep the battery charging current at 1.5A in non-MPPT mode. We can see it was successful in keeping the system stable and the transition was also quite smooth.

Next at (2) we again change the load back to 30W. The lowering DC-Link voltage triggers the mode change from non-MPPT to MPPT. The transition is smooth and the system stabilizes very quickly.

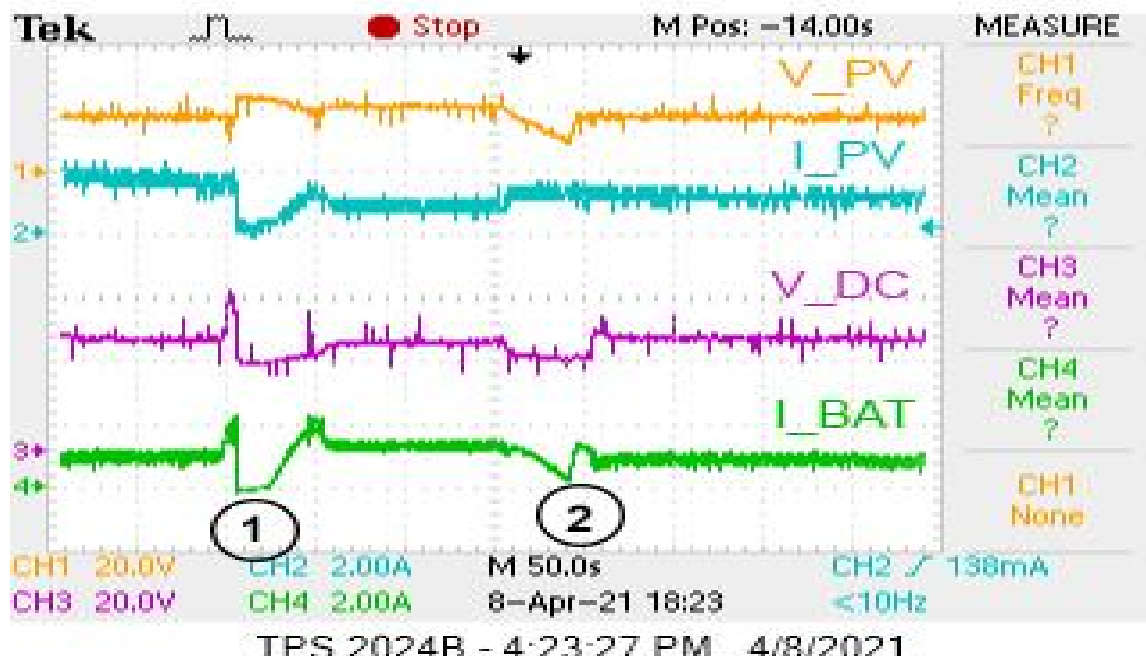


Fig. 7.1.C.1 Full waveform for mode switching from MPPT to non-MPPT to MPPT

# Chapter 8 Conclusions and Future Work

We should first discuss some major strengths of this system. Firstly the system is easy to debug thanks to the Arduino platform. This allowed us to calibrate and work on our control systems which are responsible for mode changing. These mode-changing algorithms with an exponential moving average like summer have proved to be very smooth and fast in operation despite working on an Arduino which has a limited computational capacity. Secondly, the isolation on a component level has added a good layer of security between the microcontroller and the main power circuit. Thus, this circuit protects the microcontroller from any damage due to current or voltage surges in the main circuit.

The system is observed to be working smoothly in normal operating conditions. Though we did observe that the non-MPPT mode boost controller becomes dysfunctional if there is a jerk and the voltage of the PV falls below the maximum power point (MPP). To circumvent this issue, an additional algorithm “Non-MPPT Boost” can be implemented which should take care of this issue. The control system block diagram of the proposed system is shown below.

Another issue lies with the calibration needed by the voltage sensor. Due to miscalibration, occasionally the MPPT or DC-Link Voltage Regulation does not work accurately. This issue needs further research. One of the reasons is that we rely on cheap electronics, it is easily solvable by using a voltage sensor module but that would add to the cost of the system.

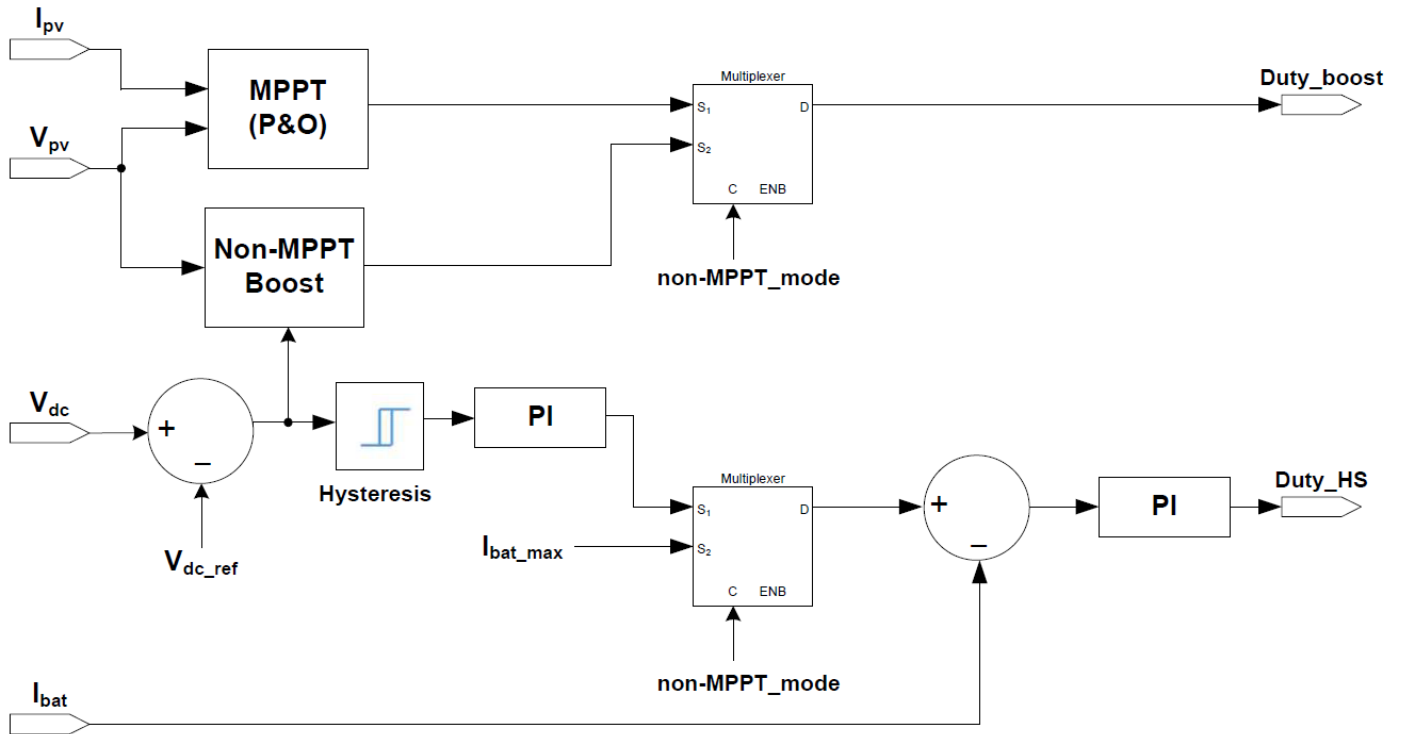


Fig. 8.1 Block diagram of modified non-MPPT Control system

Arduino, although not as expensive as a DSP, is the major expense in the project. This cost could be reduced by using a microcontroller chip directly with just the required I/O pins. Though this would take a great deal of time and effort by the programmer and debugging such systems is a tedious task. This is advised only after the prototype Arduino models are perfected.

Currently, we have set the maximum battery charging current as a constant value. However, in some previous research articles, an effort has been made to make it a function of the State of Charge (SOC). SOC itself is a function of the voltage and current of the battery. This may improve battery performance and lead to further elongation of battery life. Overall it will be a wise step and will add to the lifetime value of the system.

# References

- [1] Chattopadhyay Ritwik, and Kishore Chatterjee. "PV based stand alone single phase power generating unit." IECON 2012-38th Annual Conference on IEEE Industrial Electronics Society. IEEE, 2012.
- [2] The National Renewable Energy Laboratory, US retrieved 26th May 2021 from <https://www.nrel.gov/pv/applications.html>
- [3] How to use isolated MOSFET driver TLP250 retrieved 26th May 2021 from <https://microcontrollerslab.com/isolated-mosfet-driver-tlp250>
- [4] Ahmed, Jubaer, and Zainal Salam. "An improved perturb and observe (P&O) maximum power point tracking (MPPT) algorithm for higher efficiency." Applied Energy 150 (2015): 97-108.
- [5] ACS712, Datasheet. "Fully Integrated, Hall Effect-Based Linear Current Sensor IC with 2.1 kV RMS Isolation and a Low-Resistance Current Conductor." (2006).
- [6] Chakraborty, Suvamit, and Amod C Umarikar. "Standalone PV system based on Isolated Quasi Z-Source Converter." 2018 IEEE International Conference on Power Electronics, Drives and Energy Systems (PEDES). IEEE, 2018.
- [7] Cadence PCB solutions retrieved 27th May 2021 from <https://resourcespcb.cadence.com/blog/2020-pcb-assembly-considerations>
- [8] Bhattacharjee, Subhadeep, and Barnam Jyoti Saharia. "A comparative study on converter topologies for maximum power point tracking application in photovoltaic generation." Journal of Renewable and Sustainable Energy 6.5 (2014): 053140.

- [9] Ritwik Chattopadhyay. Chapter 3, “Stand Alone PV Based Single Phase Power Generating Unit for Rural Household Application” THESIS, Department of Electrical Engineering Indian Institute of Technology, Mumbai, July 2012.